

CHAPTER 1

DEFINITIONS AND DESIGN RELATIONS

1.1 NOTATION

a = radius of hole

a = material constant for evaluating notch sensitivity factor

a = major axis of ellipse

a = half crack length

A = area (or point)

b = minor axis of ellipse

d = diameter (or width)

D = diameter, larger diameter

h = thickness

H = width, larger width

K = stress concentration factor

K_e = effective stress concentration factor

K_f = fatigue notch factor for normal stress

K_{fs} = fatigue notch factor for shear stress

K_t = theoretical stress concentration factor for normal stress

K_{t2}, K_{t3} = stress concentration factors for two- and three-dimensional problems

K_{tf} = estimated fatigue notch factor for normal stress

K_{tsf} = estimated fatigue notch factor for shear stress

K_{tg} = stress concentration factor with the nominal stress based on gross area

K_m = stress concentration factor with the nominal stress based on net area

$K_{tx}, K_{t\theta}$ = stress concentration factors in x, θ directions

2 DEFINITIONS AND DESIGN RELATIONS

- K_{ts} = stress concentration factor for shear stress
 K'_l = stress concentration factor using a theory of failure
 K_I = mode I stress intensity factor
 l, m = direction cosines of normal to boundary
 L_b = limit design factor for bending
 M = moment
 n = factor of safety
 p = pressure
 p_x, p_y = surface forces per unit area in x, y directions
 P = load, force
 $\bar{p}_{Vx}, \bar{p}_{Vy}, \bar{p}_{Vr}$ = body forces per unit volume in x, y, r directions
 q = notch sensitivity factor
 r = radius of curvature of hole, arc, notch
 R = radius of hole, circle, or radial distance
 r, θ = polar coordinates
 r, θ, x = cylindrical coordinates
 t = depth of groove, notch
 T = torque
 u, v, w = displacements in x, y, z directions (or in r, θ, x directions in cylindrical coordinates)
 x, y, z = rectangular coordinates
 $\varepsilon_r, \varepsilon_\theta, \varepsilon_x, \gamma_{rx}$ = strain components
 ν = Poisson's ratio
 ρ = mass density
 ρ' = material constant for evaluating notch sensitivity factor
 σ = normal stress
 σ_a = alternating normal stress amplitude
 σ_n = normal stress based on net area
 σ_{eq} = equivalent stress
 σ_f = fatigue strength (endurance limit)
 σ_{max} = maximum normal stress
 σ_{nom} = nominal or reference normal stress
 σ_0 = static normal stress
 $\sigma_x, \sigma_y, \tau_{xy}$ = stress components
 $\sigma_r, \sigma_\theta, \tau_{r\theta}, \tau_{\theta r}$ = stress components
 σ_y = yield strength (tension)
 σ_{ut} = ultimate tensile strength
 σ_{uc} = ultimate compressive strength
 $\sigma_1, \sigma_2, \sigma_3$ = principal stresses
 τ = shear stress
 τ_a = alternating shear stress
 τ_f = fatigue limit in torsion

- τ_y = yield strength in torsion
 τ_{\max} = maximum shear stress
 τ_{nom} = nominal or reference shear stress
 τ_0 = static shear stress
 ω = angular rotating speed

1.2 STRESS CONCENTRATION

The elementary stress formulas used in the design of structural members are based on the members having a constant section or a section with gradual change of contour (Fig. 1.1). Such conditions, however, are hardly ever attained throughout the highly stressed region of actual machine parts or structural members. The presence of shoulders, grooves, holes, keyways, threads, and so on, results in modifications of the simple stress distributions of Fig. 1.1 so that localized high stresses occur as shown in Figs. 1.2 and 1.3. This localization of high stress is known as *stress concentration*, measured by the *stress concentration factor*. The stress concentration factor K can be defined as the ratio of the peak stress in the body (or stress in the perturbed region) to some other stress (or stresslike quantity) taken as a

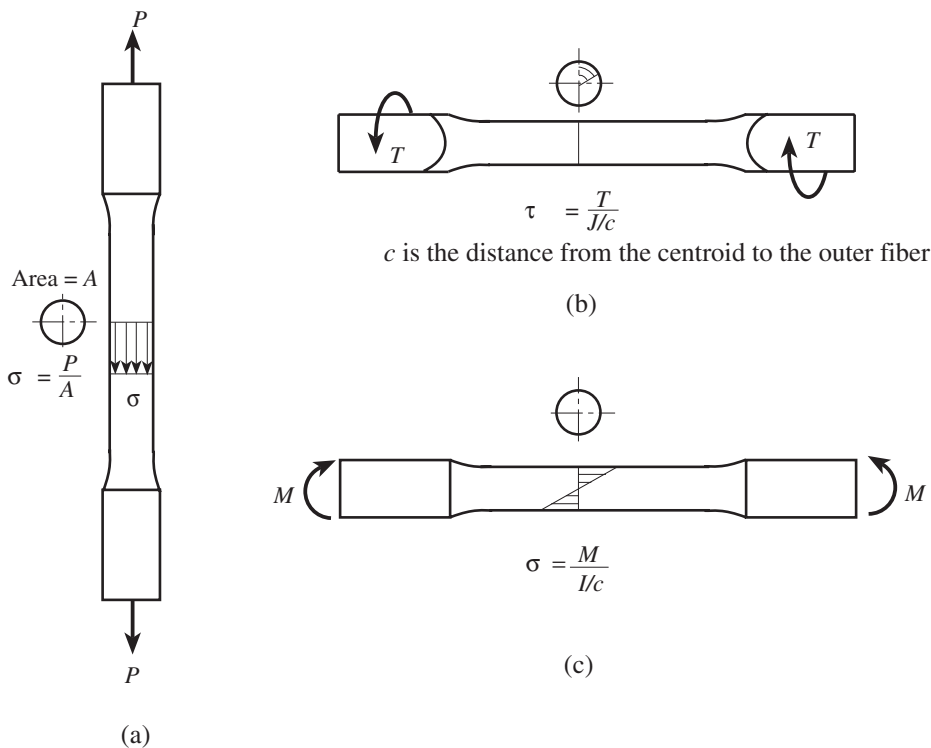


Figure 1.1 Elementary stress cases for specimens of constant cross section or with a gradual cross-sectional change: (a) tension; (b) torsion; (c) bending.

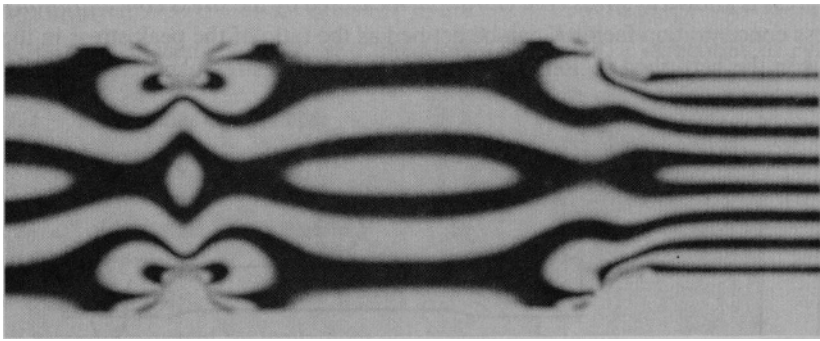
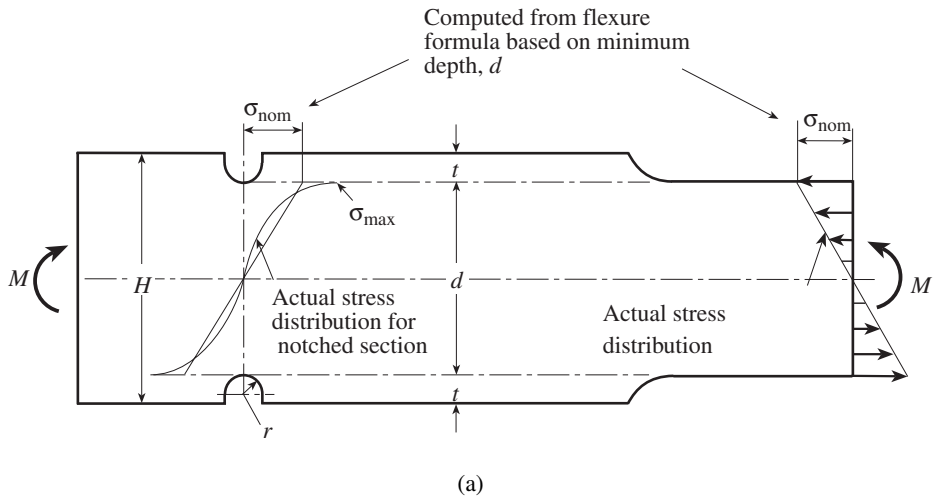


Figure 1.2 Stress concentrations introduced by a notch and a cross-sectional change which is not gradual: (a) bending of specimen; (b) photoelastic fringe photograph (Peterson 1974).

reference stress:

$$K_t = \frac{\sigma_{\max}}{\sigma_{\text{nom}}} \quad \text{for normal stress (tension or bending)} \quad (1.1)$$

$$K_{ts} = \frac{\tau_{\max}}{\tau_{\text{nom}}} \quad \text{for shear stress (torsion)} \quad (1.2)$$

where the stresses σ_{\max} , τ_{\max} represent the maximum stresses to be expected in the member under the actual loads and the *nominal stresses* σ_{nom} , τ_{nom} are reference normal and shear stresses. The subscript *t* indicates that the stress concentration factor is a theoretical factor. That is to say, the peak stress in the body is based on the theory of elasticity, or it is derived from a laboratory stress analysis experiment. The subscript *s* of Eq. (1.2) is often ignored. In the case of the theory of elasticity, a two-dimensional stress distribution of a homogeneous elastic body under known loads is a function only of the body geometry and is not dependent on the material properties. This book deals primarily with elastic stress concentration

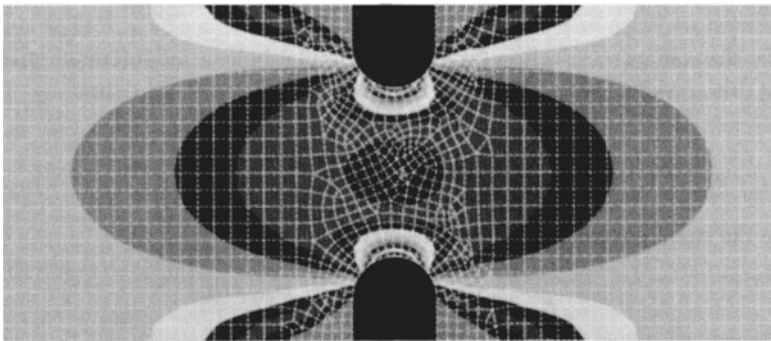
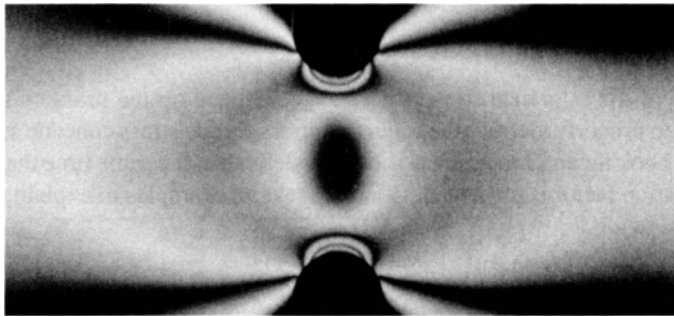
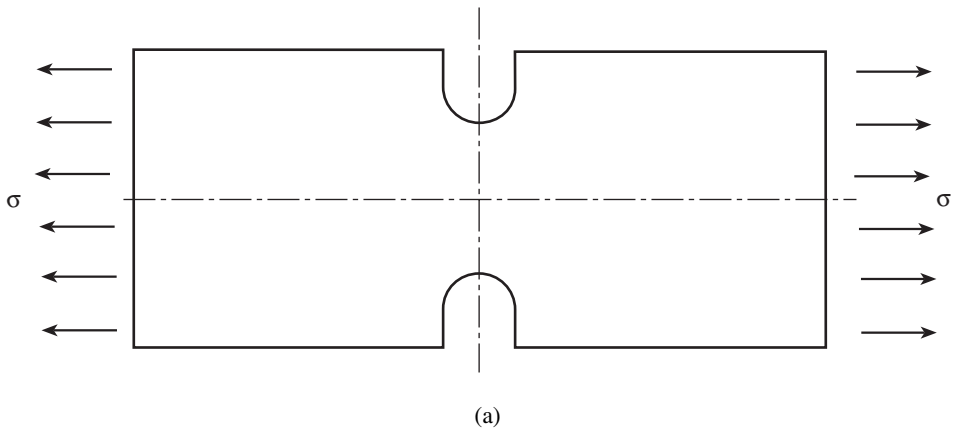


Figure 1.3 Tension bar with notches: (a) specimen; (b) photoelastic fringe photograph (Doz. Dr.-Ing. habil. K. Fethke, Universität Rostock); (c) finite element solution (Guy Neraud, University of Virginia).

factors. In the plastic range one must consider separate stress and strain concentration factors that depend on the shape of the stress-strain curve and the stress or strain level. Sometimes K_t is also referred to as a *form factor*. The subscript t distinguishes factors derived from theoretical or computational calculations, or experimental stress analysis methods such as photoelasticity, or strain gage tests from factors obtained through mechanical damage tests such as impact tests. For example, the fatigue notch factor K_f is determined using a fatigue test. It will be described later.

The universal availability of powerful, effective computational capabilities, usually based on the finite element method, has altered the use of and the need for stress concentration factors. Often a computational stress analysis of a mechanical device, including highly stressed regions, is performed as shown in Fig. 1.3c, and the explicit use of stress concentration factors is avoided. Alternatively, a computational analysis can provide the stress concentration factor, which is then available for traditional design studies. The use of experimental techniques such as photoelasticity (Fig. 1.3b) to determine stress concentration factors has been virtually replaced by the more flexible and more efficient computational techniques.

1.2.1 Selection of Nominal Stresses

The definitions of the reference stresses σ_{nom} , τ_{nom} depend on the problem at hand. It is very important to properly identify the reference stress for the stress concentration factor of interest. In this book the reference stress is usually defined at the same time that a particular stress concentration factor is presented. Consider several examples to explain the selection of reference stresses.

Example 1.1 Tension Bar with a Hole Uniform tension is applied to a bar with a single circular hole, as shown in Fig. 1.4a. The maximum stress occurs at point A, and the stress distribution can be shown to be as in Fig. 1.4a. Suppose that the thickness of the plate is h , the width of the plate is H , and the diameter of the hole is d . The reference stress could be defined in two ways:

- a. Use the stress in a cross section far from the circular hole as the reference stress. The area at this section is called the *gross cross-sectional area*. Thus define

$$\sigma_{\text{nom}} = \frac{P}{Hh} = \sigma \quad (1)$$

so that the stress concentration factor becomes

$$K_{tg} = \frac{\sigma_{\text{max}}}{\sigma_{\text{nom}}} = \frac{\sigma_{\text{max}}}{\sigma} = \frac{\sigma_{\text{max}}Hh}{P} \quad (2)$$

- b. Use the stress based on the cross section at the hole, which is formed by removing the circular hole from the gross cross section. The corresponding area is referred to as the *net cross-sectional area*. If the stresses at this cross section are uniformly distributed and equal to σ_n :

$$\sigma_n = \frac{P}{(H-d)h} \quad (3)$$

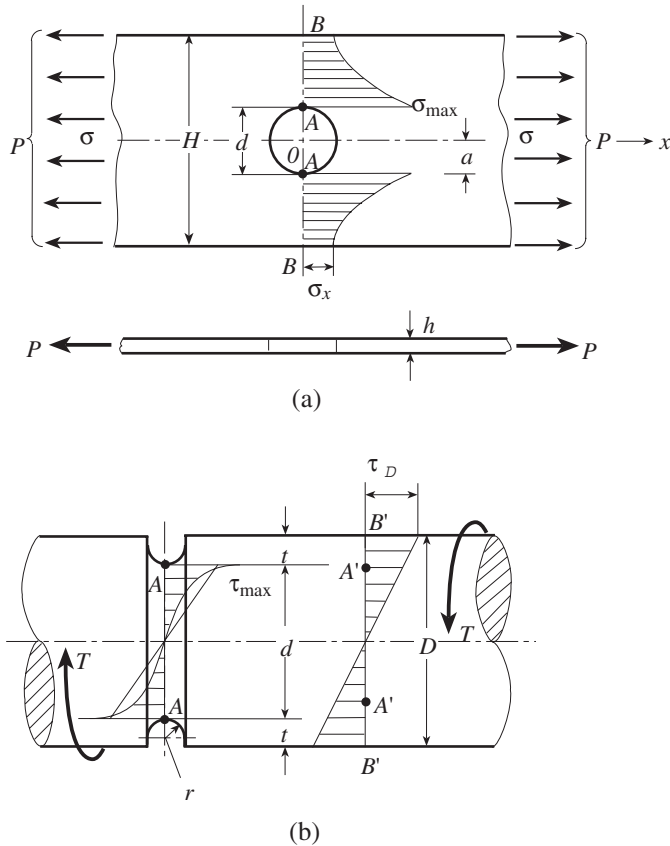


Figure 1.4 (a) Tension bar with hole; (b) torsion bar with groove.

The stress concentration factor based on the reference stress σ_n , namely, $\sigma_{\text{nom}} = \sigma_n$, is

$$K_m = \frac{\sigma_{\text{max}}}{\sigma_{\text{nom}}} = \frac{\sigma_{\text{max}}}{\sigma_n} = \frac{\sigma_{\text{max}}(H-d)h}{P} = K_{t_g} \frac{H-d}{H} \quad (4)$$

In general, K_{t_g} and K_m are different. Both are plotted in Chart 4.1. Observe that as d/H increases from 0 to 1, K_{t_g} increases from 3 to ∞ , whereas K_m decreases from 3 to 2. Either K_m or K_{t_g} can be used in calculating the maximum stress. It would appear that K_{t_g} is easier to determine as σ is immediately evident from the geometry of the bar. But the value of K_{t_g} is hard to read from a stress concentration plot for $d/H > 0.5$, since the curve becomes very steep. In contrast, the value of K_m is easy to read, but it is necessary to calculate the net cross-sectional area to find the maximum stress. Since the stress of interest is usually on the net cross section, K_m is the more generally used factor. In addition, in a fatigue analysis, only K_m can be used to calculate the stress gradient correctly. In conclusion, normally it is more convenient to give stress concentration factors using reference stresses based on the net area rather than the gross area. However, if a fatigue analysis is not involved and $d/H < 0.5$, the user may choose to use K_{t_g} to simplify calculations.

Example 1.2 Torsion Bar with a Groove A bar of circular cross section, with a U-shaped circumferential groove, is subject to an applied torque T . The diameter of the bar is D , the radius of the groove is r , and the depth of the groove is t . The stress distribution for the cross section at the groove is shown in Fig. 1.4*b*, with the maximum stress occurring at point A at the bottom of the groove. Among the alternatives to define the reference stress are:

- a. Use the stress at the outer surface of the bar cross section $B'-B'$, which is far from the groove, as the reference stress. According to basic strength of materials (Pilkey 2005), the shear stress is linearly distributed along the radial direction and

$$\tau_{B'} = \tau_D = \frac{16T}{\pi D^3} = \tau_{\text{nom}} \quad (1)$$

- b. Consider point A' in the cross section $B'-B'$. The distance of A' from the central axis is same as that of point A , that is, $d = D - 2t$. If the stress at A' is taken as the reference stress, then

$$\tau_{A'} = \frac{16Td}{\pi D^4} = \tau_{\text{nom}} \quad (2)$$

- c. Use the surface stress of a grooveless bar of diameter $d = D - 2t$ as the reference stress. This corresponds to a bar of cross section measured at $A-A$ of Fig. 1.4*b*. For this area $\pi d^2/4$, the maximum torsional stress taken as a reference stress would be

$$\tau_A = \frac{16T}{\pi d^3} = \tau_{\text{nom}} \quad (3)$$

In fact this stress based on the net area is an assumed value and never occurs at any point of interest in the bar with a U-shaped circumferential groove. However, since it is intuitively appealing and easy to calculate, it is more often used than the other two reference stresses.

Example 1.3 Cylinder with an Eccentric Hole A cylinder with an eccentric circular hole is subjected to internal pressure p as shown in Fig. 1.5. An elastic solution for stress is difficult to find. It is convenient to use the pressure p as the reference stress

$$\sigma_{\text{nom}} = p$$

so that

$$K_t = \frac{\sigma_{\text{max}}}{p}$$

These examples illustrate that there are many options for selecting a reference stress. In this book the stress concentration factors are given based on a variety of reference stresses, each of which is noted on the appropriate graph of the stress concentration factor. Sometimes, more than one stress concentration factor is plotted on a single chart. The reader should select the type of factor that appears to be the most convenient.

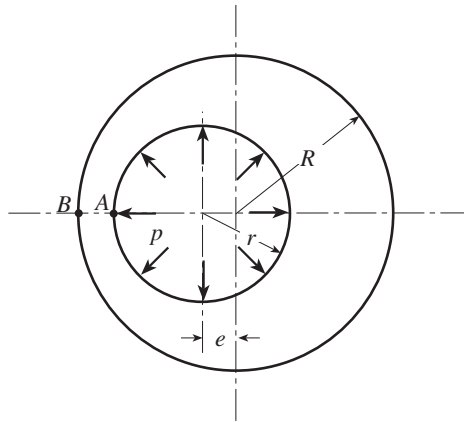


Figure 1.5 Circular cylinder with an eccentric hole.

1.2.2 Accuracy of Stress Concentration Factors

Stress concentration factors are obtained analytically from the elasticity theory, computationally from the finite element method, and experimentally using methods such as photoelasticity or strain gages. For torsion, the membrane analogy (Pilkey and Wunderlich 1993) can be employed. When the experimental work is conducted with sufficient precision, excellent agreement is often obtained with well-established analytical stress concentration factors.

Unfortunately, use of stress concentration factors in analysis and design is not on as firm a foundation as the theoretical basis for determining the factors. The theory of elasticity solutions are based on formulations that include such assumptions as that the material must be isotropic and homogeneous. However, in actuality materials may be neither uniform nor homogeneous, and may even have defects. More data are necessary because, for the required precision in material tests, statistical procedures are often necessary. Directional effects in materials must also be carefully taken into account. It is hardly necessary to point out that the designer cannot wait for exact answers to all of these questions. As always, existing information must be reviewed and judgment used in developing reasonable approximate procedures for design, tending toward the safe side in doubtful cases. In time, advances will take place and revisions in the use of stress concentration factors will need to be made accordingly. On the other hand, it can be said that our limited experience in using these methods has been satisfactory.

1.2.3 Decay of Stress Away from the Peak Stress

There are a number of theories of elasticity analytical solutions for stress concentrations, such as for an elliptical hole in a panel under tension. As can be observed in Fig. 1.4a, these solutions show that typically, the stress decays approximately exponentially from the location of the peak stresses to the nominal value at a remote location, with the rate of decay higher near the peak value of stress.

1.3 STRESS CONCENTRATION AS A TWO-DIMENSIONAL PROBLEM

Consider a thin element lying in the x, y plane, loaded by in-plane forces applied in the x, y plane at the boundary (Fig. 1.6a). For this case the stress components $\sigma_z, \tau_{xz}, \tau_{yz}$ can be assumed to be equal to zero. This state of stress is called *plane stress*, and the stress components $\sigma_x, \sigma_y, \tau_{xy}$ are functions of x and y only. If the dimension in the z direction of a long cylindrical or prismatic body is very large relative to its dimensions in the x, y plane and the applied forces are perpendicular to the longitudinal direction (z direction) (Fig. 1.6b), it may be assumed that at the midsection the z direction strains ϵ_z, γ_{xz} , and γ_{yz} are equal to zero. This is called the *plane strain* state. These two-dimensional problems are referred to as *plane problems*.

The differential equations of equilibrium together with the compatibility equation for the stresses $\sigma_x, \sigma_y, \tau_{xy}$ in a plane elastic body are (Pilkey and Wunderlich 1993)

$$\begin{aligned} \frac{\partial \sigma_x}{\partial x} + \frac{\partial \tau_{xy}}{\partial y} + \bar{p}_{Vx} &= 0 \\ \frac{\partial \tau_{xy}}{\partial x} + \frac{\partial \sigma_y}{\partial y} + \bar{p}_{Vy} &= 0 \end{aligned} \tag{1.3}$$

$$\left(\frac{\partial^2}{\partial x^2} + \frac{\partial^2}{\partial y^2} \right) (\sigma_x + \sigma_y) = -f(\nu) \left(\frac{\partial \bar{p}_{Vx}}{\partial x} + \frac{\partial \bar{p}_{Vy}}{\partial y} \right) \tag{1.4}$$

where $\bar{p}_{Vx}, \bar{p}_{Vy}$ denote the components of the applied body force per unit volume in the x, y directions and $f(\nu)$ is a function of Poisson's ratio:

$$f(\nu) = \begin{cases} 1 + \nu & \text{for plane stress} \\ \frac{1}{1 - \nu} & \text{for plane strain} \end{cases}$$

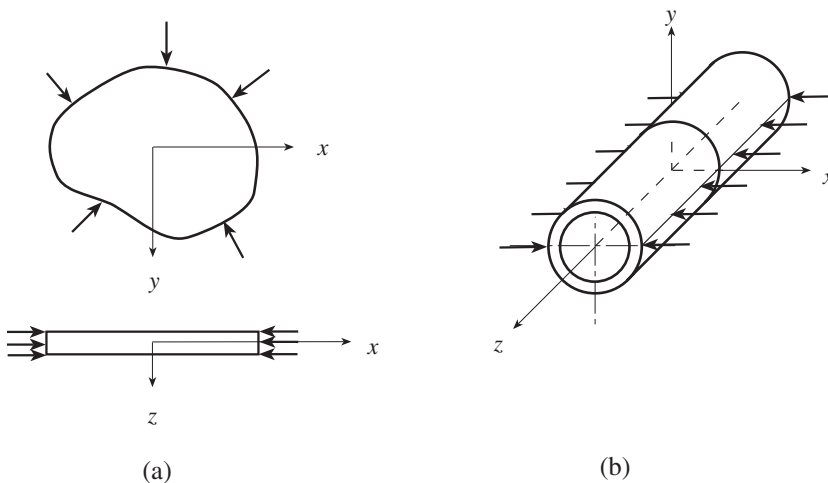


Figure 1.6 (a) Plane stress; (b) plane strain.

The surface conditions are

$$\begin{aligned} p_x &= l\sigma_x + m\tau_{xy} \\ p_y &= l\tau_{xy} + m\sigma_y \end{aligned} \quad (1.5)$$

where p_x, p_y are the components of the surface force per unit area at the boundary in the x, y directions. Also, l, m are the direction cosines of the normal to the boundary. For constant body forces, $\partial \bar{p}_{Vx}/\partial x = \partial \bar{p}_{Vy}/\partial y = 0$, and Eq. (1.4) becomes

$$\left(\frac{\partial^2}{\partial x^2} + \frac{\partial^2}{\partial y^2} \right) (\sigma_x + \sigma_y) = 0 \quad (1.6)$$

Equations (1.3), (1.5), and (1.6) are usually sufficient to determine the stress distribution for two-dimensional problems with constant body forces. These equations do not contain material constants. For plane problems, if the body forces are constant, the stress distribution is a function of the body shape and loadings acting on the boundary and not of the material. This implies for plane problems that stress concentration factors are functions of the geometry and loading and not of the type of material. Of practical importance is that stress concentration factors can be found using experimental techniques such as photoelasticity that utilize material different from the structure of interest.

1.4 STRESS CONCENTRATION AS A THREE-DIMENSIONAL PROBLEM

For three-dimensional problems, there are no simple relationships similar to Eqs. (1.3), (1.5), and (1.6) for plane problems that show the stress distribution to be a function of body shape and applied loading only. In general, the stress concentration factors will change with different materials. For example, Poisson's ratio ν is often involved in a three-dimensional stress concentration analysis. In this book most of the charts for three-dimensional stress concentration problems not only list the body shape and load but also the Poisson's ratio ν for the case. The influence of Poisson's ratio on the stress concentration factors varies with the configuration. For example, in the case of a circumferential groove in a round bar under torsional load (Fig. 1.7), the stress distribution and concentration factor do not depend on Poisson's ratio. This is because the shear deformation due to torsion does not change the volume of the element, namely the cross-sectional areas remain unchanged.

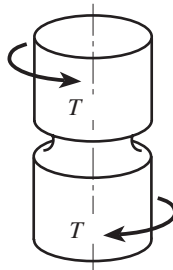


Figure 1.7 Round bar with a circumferential groove and torsional loading.

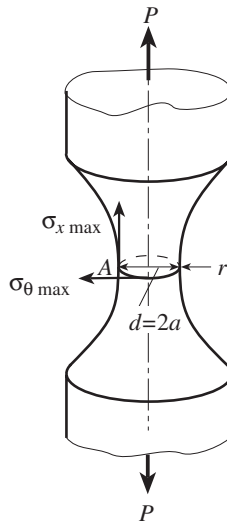


Figure 1.8 Hyperbolic circumferential groove in a round bar.

As another example, consider a hyperbolic circumferential groove in a round bar under tension load P (Fig. 1.8). The stress concentration factor in the axial direction is (Neuber 1958)

$$K_{tx} = \frac{\sigma_{x \max}}{\sigma_{\text{nom}}} = \frac{1}{(a/r) + 2\nu C + 2} \left[\frac{a}{r}(C + \nu + 0.5) + (1 + \nu)(C + 1) \right] \quad (1.7)$$

and in the circumferential direction is

$$K_{t\theta} = \frac{\sigma_{\theta \max}}{\sigma_{\text{nom}}} = \frac{a/r}{(a/r) + 2\nu C + 2} (\nu C + 0.5) \quad (1.8)$$

where r is the radius of curvature at the base of the groove, C is $\sqrt{(a/r) + 1}$, and the reference stress σ_{nom} is $P/(\pi a^2)$. Obviously K_{tx} and $K_{t\theta}$ are functions of ν . Table 1.1 lists the stress concentration factors for different Poisson's ratios for the hyperbolic circumferential groove when $a/r = 7.0$. From this table it can be seen that as the value of ν increases, K_{tx} decreases slowly whereas $K_{t\theta}$ increases relatively rapidly. When $\nu = 0$, $K_{tx} = 3.01$ and $K_{t\theta} = 0.39$. It is interesting that when Poisson's ratio is equal to zero (there is no transverse contraction in the round bar), the maximum circumferential stress $\sigma_{\theta \max}$ is not equal to zero.

TABLE 1.1 Stress Concentration Factor as a Function of Poisson's Ratio for a Shaft in Tension with a Groove^a

ν	0.0	0.1	0.2	0.3	0.4	≈ 0.5
K_{tx}	3.01	2.95	2.89	2.84	2.79	2.75
$K_{t\theta}$	0.39	0.57	0.74	0.88	1.01	1.13

^aThe shaft has a hyperbolic circumferential groove with $a/r = 7.0$.

1.5 PLANE AND AXISYMMETRIC PROBLEMS

For a solid of revolution deformed symmetrically with respect to the axis of revolution, it is convenient to use cylindrical coordinates (r, θ, x) . The stress components are independent of the angle θ and $\tau_{r\theta}, \tau_{\theta x}$ are equal to zero. The equilibrium and compatibility equations for the axisymmetrical case are (Timoshenko and Goodier 1970)

$$\frac{\partial \sigma_r}{\partial r} + \frac{\partial \tau_{rx}}{\partial x} + \frac{\sigma_r - \sigma_\theta}{r} + \bar{p}_{Vr} = 0 \tag{1.9}$$

$$\frac{\partial \tau_{rx}}{\partial r} + \frac{\partial \sigma_x}{\partial x} + \frac{\tau_{rx}}{r} + \bar{p}_{Vx} = 0$$

$$\frac{\partial^2 \epsilon_r}{\partial x^2} + \frac{\partial^2 \epsilon_x}{\partial r^2} = \frac{\partial^2 \gamma_{rx}}{\partial r \partial x} \tag{1.10}$$

The strain components are

$$\epsilon_r = \frac{\partial u}{\partial r}, \quad \epsilon_\theta = \frac{u}{r}, \quad \epsilon_x = \frac{\partial w}{\partial x}, \quad \gamma_{rx} = \frac{\partial u}{\partial x} + \frac{\partial w}{\partial r} \tag{1.11}$$

where u and w are the displacements in the r (radial) and x (axial) directions, respectively. The axisymmetric stress distribution in a solid of revolution is quite similar to the stress distribution for a two-dimensional plane element, the shape of which is the same as a longitudinal section of the solid of revolution (see Fig. 1.9). Strictly speaking, their stress distributions and stress concentration factors should not be equal. But under certain circumstances, their stress concentration factors are very close. To understand the relationship between plane and axisymmetric problems, consider the following cases.

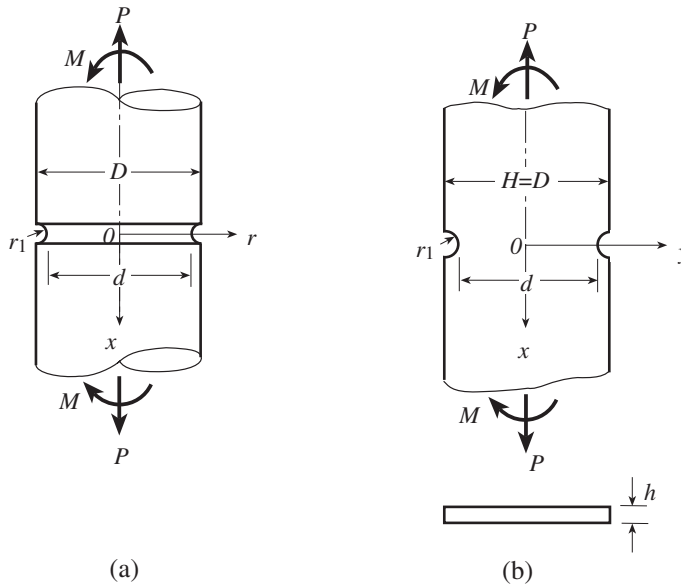


Figure 1.9 Shaft with a circumferential groove and a plane element with the same longitudinal sectional shape: (a) shaft, K_{t3} ; (b) plane, K_{t2} .

CASE 1. *A Shaft with a Circumferential Groove and with the Stress Raisers Far from the Central Axis of Symmetry* Consider a shaft with a circumferential groove under tension (or bending) load, and suppose the groove is far from the central axis, $d/2 \gg r_1$, as shown in Fig. 1.9a. A plane element with the same longitudinal section under the same loading is shown in Fig 1.9b. Let K_{t3} and K_{t2} denote the stress concentration factors for the axisymmetric solid body and the corresponding plane problem, respectively. Since the groove will not affect the stress distribution in the area near the central axis, the distributions of stress components σ_x , σ_r , τ_{xr} near the groove in the axisymmetric shaft are almost the same as those of the stress components σ_x , σ_y , τ_{xy} near the notch in the plane element, so that $K_{t3} \approx K_{t2}$.

For the case where a small groove is a considerable distance from the central axis of the shaft, the same conclusion can be explained as follows. Set the terms with $1/r$ equal to 0 (since the groove is far from the central axis, r is very large), and note that differential Eqs. (1.9) reduce to

$$\begin{aligned} \frac{\partial \sigma_r}{\partial r} + \frac{\partial \tau_{rx}}{\partial x} + \bar{p}_{Vr} &= 0 \\ \frac{\partial \tau_{rx}}{\partial r} + \frac{\partial \sigma_x}{\partial x} + \bar{p}_{Vx} &= 0 \end{aligned} \quad (1.12)$$

and Eq. (1.11) becomes

$$\varepsilon_r = \frac{\partial u}{\partial r}, \quad \varepsilon_\theta = 0, \quad \varepsilon_x = \frac{\partial w}{\partial x}, \quad \gamma_{rx} = \frac{\partial u}{\partial x} + \frac{\partial w}{\partial r} \quad (1.13)$$

Introduce the material law

$$\begin{aligned} \varepsilon_r &= \frac{1}{E}[\sigma_r - \nu(\sigma_\theta + \sigma_x)], \quad \varepsilon_\theta = 0 = \frac{1}{E}[\sigma_\theta - \nu(\sigma_x + \sigma_r)] \\ \varepsilon_x &= \frac{1}{E}[\sigma_x - \nu(\sigma_r + \sigma_\theta)], \quad \gamma_{rx} = \frac{1}{G}\tau_{rx} \end{aligned}$$

into Eq. (1.10) and use Eq. (1.12). For constant body forces this leads to an equation identical (with y replaced by r) to that of Eq. (1.6). This means that the governing equations are the same. However, the stress σ_θ is not included in the governing equations and it can be derived from

$$\sigma_\theta = \nu(\sigma_r + \sigma_x) \quad (1.14)$$

When $\nu = 0$, the stress distribution of a shaft is identical to that of the plane element with the same longitudinal section.

CASE 2. *General Case of an Axisymmetrical Solid with Shallow Grooves and Shoulders* In general, for a solid of revolution with shallow grooves or shoulders under tension or bending as shown in Fig. 1.10, the stress concentration factor K_{t3} can be obtained in terms of the plane case factor K_{t2} using (Nishida 1976)

$$\left(1 + \frac{2t}{d}\right) K_{t3} - K_{t2} = \frac{t}{d} \left(1 + \sqrt{\frac{2t}{r_1}}\right) \quad (1.15)$$

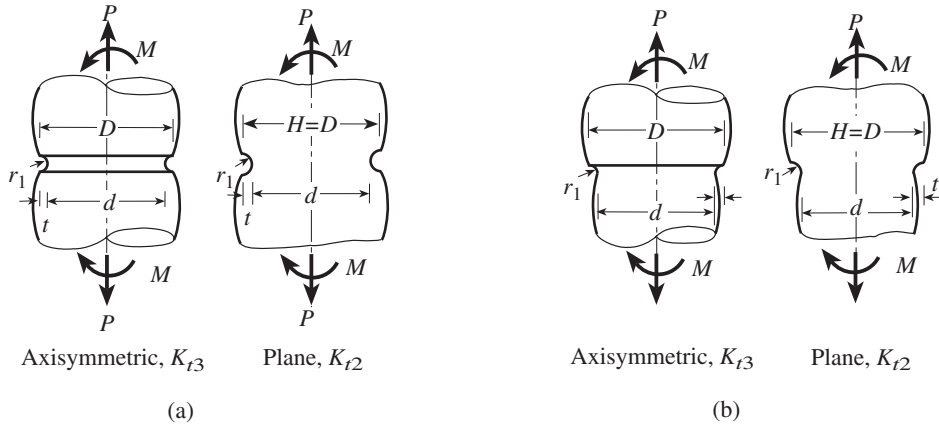


Figure 1.10 Shallow groove (a) and shoulder (b).

where r_1 is the radius of the groove and $t = (D - d)/2$ is the depth of the groove (or shoulder). The effective range for Eq. (1.15) is $0 \leq t/d \leq 7.5$. If the groove is far from the central axis, $t/d \rightarrow 0$ and $K_{t3} = K_{t2}$, which is consistent with the results discussed in Case 1.

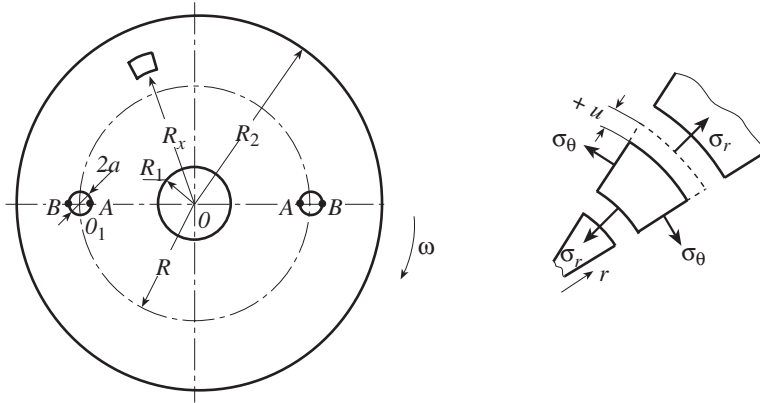
CASE 3. Deep Hyperbolic Groove As mentioned in Section 1.4, Neuber (1958) provided formulas for bars with deep hyperbolic grooves. For the case of an axisymmetric shaft under tensile load, for which the minimum diameter of the shaft d (Fig. 1.8) is smaller than the depth of the groove, the following empirical formula is available (Nishida 1976):

$$K_{t3} = 0.75K_{t2} + 0.25 \tag{1.16}$$

Equation (1.16) is close to the theoretical value over a wide range and is useful in engineering analysis. This equation not only applies to tension loading but also to bending and shearing load. However, the error tends to be relatively high in the latter cases.

1.6 LOCAL AND NONLOCAL STRESS CONCENTRATION

If the dimensions of a stress raiser are much smaller than those of the structural member, its influence is usually limited to a localized area (or volume for a three-dimensional case). That is, the global stress distribution of the member except for the localized area is the same as that for the member without the stress raiser. This kind of problem is referred to as *localized stress concentration*. Usually stress concentration theory deals with the *localized stress concentration* problems. The simplest way to solve these problems is to separate this localized part from the member, then to determine K_t by using the formulas and curves of a simple case with a similar raiser shape and loading. If a wide stress field is affected, the problem is called *nonlocal stress concentration* and can be quite complicated. Then a full-fledged stress analysis of the problem may be essential, probably with general-purpose structural analysis computer software.



- R_1 Radius of central hole R_2 Outer radius of the disk
- R Distance between the center of the disk and the center of O_1
- R_x Radius at which σ_r, σ_θ are to be calculated.
- a Radius of hole O_1 r, θ Polar coordinates

Figure 1.11 Rotating disk with a central hole and two symmetrically located holes.

Example 1.4 Rotating Disk A disk rotating at speed ω has a central hole and two additional symmetrically located holes as shown in Fig. 1.11. Suppose that $R_1 = 0.24R_2$, $a = 0.06R_2$, $R = 0.5R_2$, $\nu = 0.3$. Determine the stress concentration factor near the small circle O_1 .

Since $R_2 - R_1$ is more than 10 times greater than a , it can be reasoned that the existence of the small O_1 hole will not affect the general stress distribution. That is to say, the disruption in stress distribution due to circle O_1 is limited to a local area. This qualifies then as localized stress concentration.

For a rotating disk with a central hole, the theory of elasticity gives the stress components (Pilkey 2005)

$$\sigma_r = \frac{3 + \nu}{8} \rho \omega^2 \left(R_2^2 + R_1^2 - \frac{R_1^2 R_2^2}{R_x^2} - R_x^2 \right)$$

$$\sigma_\theta = \frac{3 + \nu}{8} \rho \omega^2 \left(R_2^2 + R_1^2 + \frac{R_1^2 R_2^2}{R_x^2} - \frac{1 + 3\nu}{3 + \nu} R_x^2 \right)$$
(1)

where ω is the speed of rotation (rad/s), ρ is the mass density, and R_x is the radius at which σ_r, σ_θ are to be calculated.

The O_1 hole may be treated as if it were in an infinite region and subjected to biaxial stresses σ_r, σ_θ as shown in Fig. 1.12a. For point A, $R_A = R - a = 0.5R_2 - 0.06R_2 = 0.44R_2$, and the elasticity solution of (1) gives

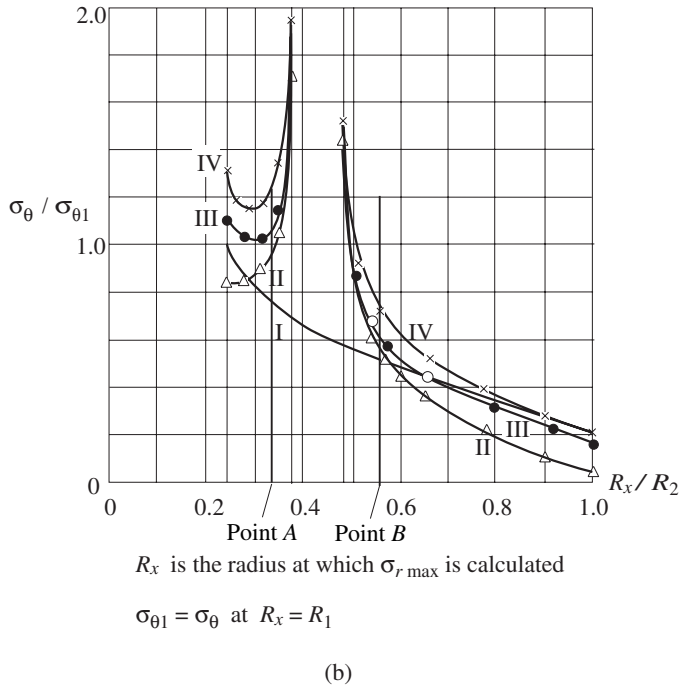
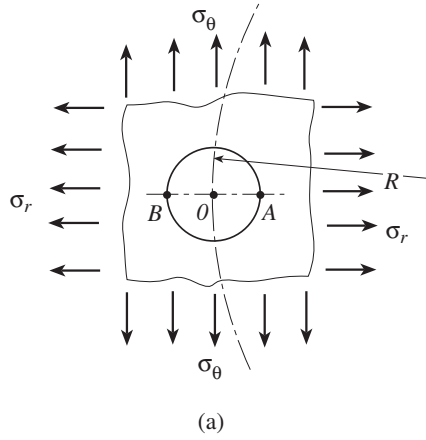


Figure 1.12 Analysis of a hollow rotating disk with two holes: (a) hole O_1 is treated as being subjected to biaxial stresses σ_r , σ_θ ; (b) results from Ku (1960). (I) No central hole; (II) approximate solution; (III) exact solution; (IV) photoelastic results (Newton 1940).

$$\begin{aligned}
 \sigma_{rA} &= \frac{3 + \nu}{8} \rho \omega^2 R_2^2 \left(1 + 0.24^2 - \frac{0.24^2}{0.44^2} - 0.44^2 \right) = 0.566 \left(\frac{3 + \nu}{8} \rho \omega^2 R_2^2 \right) \\
 \sigma_{\theta A} &= \frac{3 + \nu}{8} \rho \omega^2 R_2^2 \left(1 + 0.24^2 + \frac{0.24^2}{0.44^2} - \frac{1 + 3\nu}{3 + \nu} 0.44^2 \right) \\
 &= 1.244 \left(\frac{3 + \nu}{8} \rho \omega^2 R_2^2 \right)
 \end{aligned} \tag{2}$$

Substitute $\alpha = \sigma_{rA}/\sigma_{\theta A} = 0.566/1.244 = 0.455$ into the stress concentration factor formula for the case of an element with a circular hole under biaxial tensile load (Eq. 4.18) giving

$$K_{tA} = \frac{\sigma_{A \max}}{\sigma_{\theta A}} = 3 - 0.455 = 2.545$$

and the maximum stress at point A is

$$\sigma_{A \max} = K_{tA} \cdot \sigma_{\theta A} = 3.1660 \left(\frac{3 + \nu}{8} \rho \omega^2 R_2^2 \right) \quad (3)$$

Similarly, at point B , $R_B = R + a = 0.5R_2 + 0.06R_2 = 0.56R_2$,

$$\begin{aligned} \sigma_{rB} &= 0.56 \left(\frac{3 + \nu}{8} \rho \omega^2 R_2^2 \right) \\ \sigma_{\theta B} &= 1.061 \left(\frac{3 + \nu}{8} \rho \omega^2 R_2^2 \right) \end{aligned} \quad (4)$$

Substitute $\alpha = \sigma_{rB}/\sigma_{\theta B} = 0.56/1.061 = 0.528$ into the stress concentration factor formula of Eq. (4.18):

$$K_{tB} = \frac{\sigma_{B \max}}{\sigma_{\theta B}} = 3 - 0.528 = 2.472$$

and the maximum stress at point B becomes

$$\sigma_{B \max} = K_{tB} \cdot \sigma_{\theta B} = 2.6228 \left(\frac{3 + \nu}{8} \rho \omega^2 R_2^2 \right) \quad (5)$$

To calculate the stress at the edge of the central hole, substitute $R_x = R_1 = 0.24R_2$ into σ_{θ} of (1):

$$\sigma_{\theta 1} = 2.204 \left(\frac{3 + \nu}{8} \rho \omega^2 R_2^2 \right) \quad (6)$$

Equations (3) and (5) give the maximum stresses at points A and B of an infinite region as shown in Fig. 1.12a. If $\sigma_{\theta 1}$ is taken as the reference stress, the corresponding stress concentration factors are

$$\begin{aligned} K_{t1A} &= \frac{\sigma_{A \max}}{\sigma_{\theta 1}} = \frac{3.1660}{2.204} = 1.44 \\ K_{t1B} &= \frac{\sigma_{B \max}}{\sigma_{\theta 1}} = \frac{2.6228}{2.204} = 1.19 \end{aligned} \quad (7)$$

This approximation of treating the hole as if it were in an infinite region and subjected to biaxial stresses is based on the assumption that the influence of circle O_1 is limited to a local area. The results are very close to the theoretical solution. Ku (1960)

analyzed the case with $R_1 = 0.24R_2$, $R = 0.435R_2$, $a = 0.11R_2$. Although the circle O_1 is larger than that of this example, he still obtained reasonable approximations by treating the hole as if it were in an infinite region and subjected to biaxial stresses. The results are given in Fig. 1.12*b*, in which $\sigma_{\theta 1}$ on the central circle ($R_1 = 0.24R_2$) was taken as the reference stress. Curve II was obtained by the approximation of this example and curve III is from the theoretical solution (Howland 1930). For point A, $r/R_2 = 0.335$ and for point B, $r/R_2 = 0.545$. From Fig. 1.12*b*, it can be seen that at points A and B of the edge of hole O_1 , the results from curves II and III are very close.

The method used in Example 1.4 can be summarized as follows: First, find the stress field in the member without the stress raiser at the position where the stress raiser occurs. This analysis provides the loading condition at this local point. Second, find a formula or curve from the charts in this book that applies to the loading condition and the stress raiser shape. Finally, use the formula or curve to evaluate the maximum stress. It should be remembered that this method is only applicable for localized stress concentration.

1.6.1 Examples of Reasonable Approximations

Consider now the concept of localized stress concentration for the study of the stress caused by notches and grooves. Begin with a thin flat element with a shallow notch under uniaxial tension load as shown in Fig. 1.13*a*. Since the notch is shallow, the bottom edge of the element is considered to be a substantial distance from the notch. It is a local stress concentration problem in the vicinity of the notch. Consider another element with an elliptic hole loaded by uniaxial stress σ as indicated in Fig. 1.13*b*. (The solution for this problem can be derived from Eq. 4.58.) Cut the second element with the symmetrical axis A–A'. The normal stresses on section A–A' are small and can be neglected. Then the solution for an element with an elliptical hole (Eq. 4.58 with a replaced by t)

$$K_t = 1 + 2\sqrt{\frac{t}{r}} \tag{1.17}$$

can be taken as an approximate solution for an element with a shallow notch. According to this approximation, the stress concentration factor for a shallow notch is a function only of the depth t and radius of curvature r of the notch.

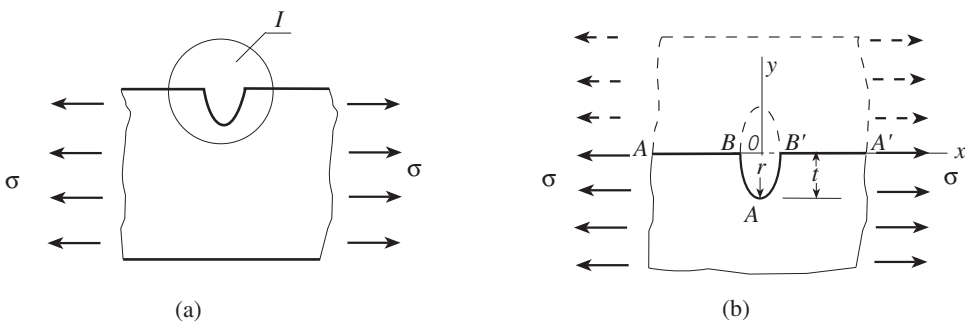


Figure 1.13 (a) Shallow groove I ; (b) model of I .

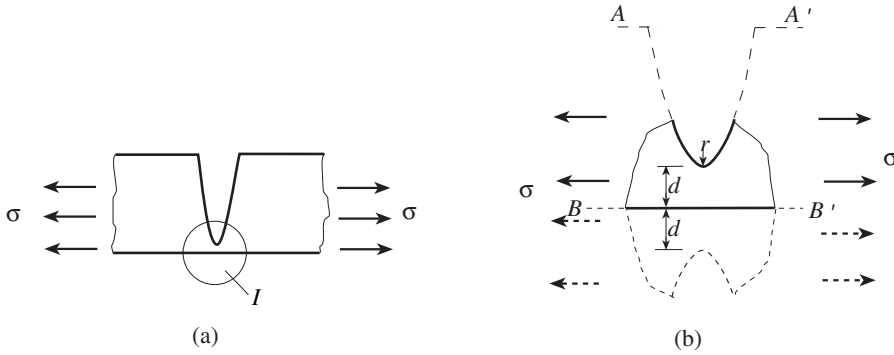


Figure 1.14 (a) Deep groove in tension; (b) model of I.

For a deep notch in a plane element under uniaxial tension load (Fig. 1.14a), the situation is quite different. For the enlarged model of Fig. 1.14b, the edge $A-A'$ is considered to be a substantial distance from bottom edge $B-B'$, and the stresses near the $A-A'$ edge are almost zero. Such a low stress area probably can be safely neglected. The local areas that should be considered are the bottom of the groove and the straight line edge $B-B'$ close to the groove bottom. Thus the deep notch problem, which might appear to be a nonlocal stress concentration problem, can also be considered as localized stress concentration. Furthermore the bottom part of the groove can be approximated by a hyperbola, since it is a small segment. Because of symmetry (Fig. 1.14) it is reasoned that the solution to this problem is same as that of a plane element with two opposing hyperbola notches. The equation for the stress concentration factor is (Durelli 1982)

$$K_t = \frac{2 \left(\frac{d}{r} + 1 \right) \sqrt{\frac{d}{r}}}{\left(\frac{d}{r} + 1 \right) \arctan \sqrt{\frac{d}{r}} + \sqrt{\frac{d}{r}}} \quad (1.18)$$

where d is the distance between the notch and edge $B-B'$ (Fig. 1.14b). It is evident that the stress concentration factor of the deep notch is a function of the radius of curvature r of the bottom of the notch and the minimum width d of the element (Fig. 1.14). For notches of intermediate depth, refer to the Neuber method (see Eq. 2.1).

1.7 MULTIPLE STRESS CONCENTRATION

Two or more stress concentrations occurring at the same location in a structural member are said to be in a state of *multiple stress concentration*. Multiple stress concentration problems occur often in engineering design. An example would be a uniaxially tension-loaded plane element with a circular hole, supplemented by a notch at the edge of the hole as shown in Fig. 1.15. The notch will lead to a higher stress than would occur with the hole alone. Use K_{t1} to represent the stress concentration factor of the element with a circular hole and K_{t2} to represent the stress concentration factor of a thin, flat tension element with a notch on an edge. In general, the multiple stress concentration factor of the element $K_{t1,2}$ cannot be

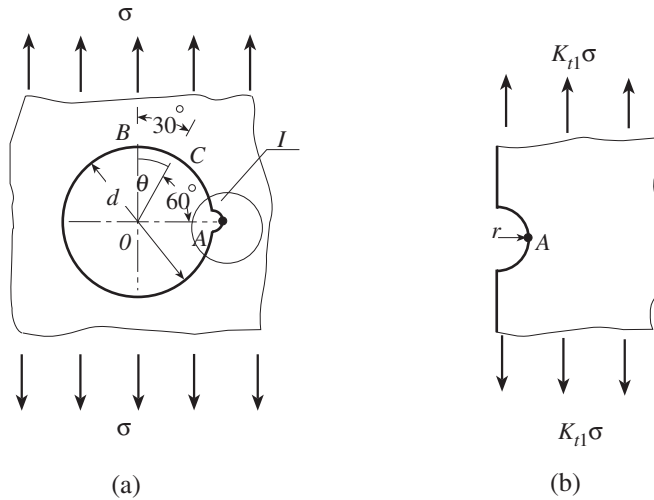


Figure 1.15 Multiple stress concentration: (a) small notch at the edge of a circular hole; (b) enlargement of I .

deduced directly from K_{t1} and K_{t2} . The two different factors will interact with each other and produce a new stress distribution. Because of its importance in engineering design, considerable effort has been devoted to finding solutions to the multiple stress concentration problems. Some special cases of these problems follow.

CASE 1. Geometrical Dimension of One Stress Raiser Much Smaller Than That of the Other Assume that $d/2 \gg r$ in Fig. 1.15, where r is the radius of curvature of the notch. Notch r will not significantly influence the global stress distribution in the element with the circular hole. However, the notch can produce a local disruption in the stress field of the element with the hole. For an infinite element with a circular hole, the stress concentration factor K_{t1} is 3.0, and for the element with a semicircular notch K_{t2} is 3.06 (Chapter 2). Since the notch does not affect significantly the global stress distribution near the circular hole, the stress around the notch region is approximately $K_{t1}\sigma$. Thus the notch can be considered to be located in a tensile specimen subjected to a tensile load $K_{t1}\sigma$ (Fig. 1.15b). Therefore the peak stress at the tip of the notch is $K_{t2} \cdot K_{t1}\sigma$. It can be concluded that the multiple stress concentration factor at point A is equal to the product of K_{t1} and K_{t2} ,

$$K_{t1,2} = K_{t1} \cdot K_{t2} = 9.18 \tag{1.19}$$

which is close to the value displayed in Chart 4.60 for $r/d \rightarrow 0$. If the notch is relocated to point B instead of A, the multiple stress concentration factor will be different. Since at point B the stress concentration factor due to the hole is -1.0 (refer to Fig. 4.4), $K_{t1,2} = -1.0 \cdot 3.06 = -3.06$. Using the same argument, when the notch is situated at point C ($\theta = \pi/6$), $K_{t2} = 0$ (refer to Section 4.3.1 and Fig. 4.4) and $K_{t1,2} = 0 \cdot 3.06 = 0$. It is evident that the stress concentration factor can be effectively reduced by placing the notch at point C.

Consider a shaft with a circumferential groove subject to a torque T , and suppose that there is a small radial cylindrical hole at the bottom of the groove as shown in Fig. 1.16.

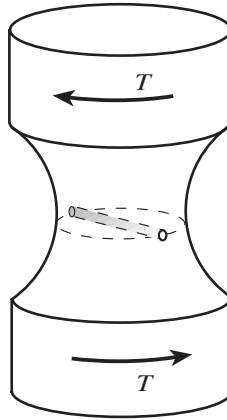


Figure 1.16 Small radial hole through a groove.

(If there were no hole, the state of stress at the bottom of the groove would be one of pure shear, and K_{s1} for this location could be found from Chart 2.47.) The stress concentration near the small radial hole can be modeled using an infinite element with a circular hole under shearing stress. Designate the corresponding stress concentration factor as K_{s2} . (Then K_{s2} can be found from Chart 4.97, with $a = b$.) The multiple stress concentration factor at the edge of the hole is

$$K_{t1,2} = K_{s1} \cdot K_{s2} \tag{1.20}$$

CASE 2. Size of One Stress Raiser Not Much Different from the Size of the Other Stress Raiser Under such circumstances the multiple stress concentration factor cannot be calculated as the product of the separate stress concentration factors as in Eq. (1.19) or (1.20). In the case of Fig. 1.17, for example, the maximum stress location A_1 for stress concentration factor 1 does not coincide with the maximum stress location A_2 for stress concentration

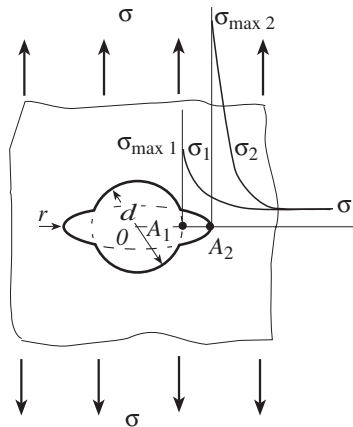


Figure 1.17 Two stress raisers of almost equal magnitude in an infinite two-dimensional element.

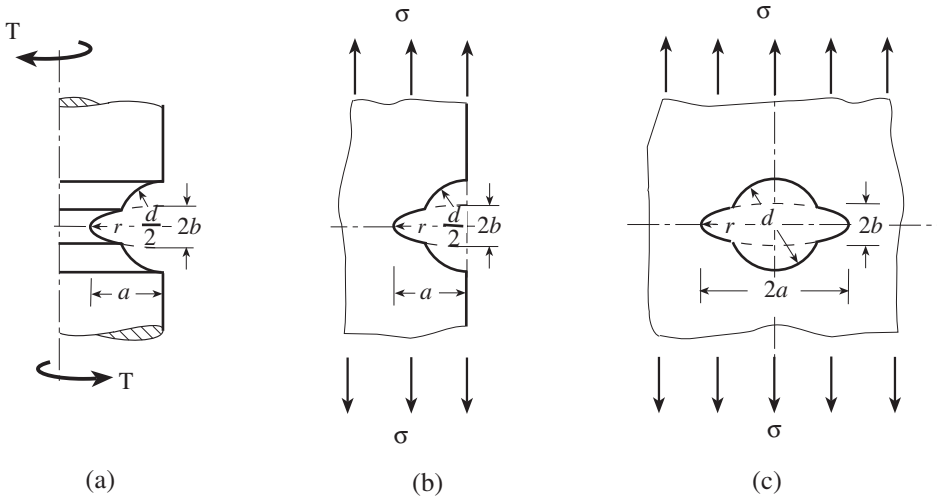


Figure 1.18 Special cases of multiple stress concentration: (a) shaft with double grooves; (b) semi-infinite element with double notches; (c) circular hole with elliptical notches.

factor 2. In general, the multiple stress concentration factor adheres to the relationship (Nishida 1976)

$$\max(K_{t1}, K_{t2}) < K_{t1,2} \leq K_{t1} \cdot K_{t2} \tag{1.21}$$

Some approximate formulas are available for special cases. For the three cases of Fig. 1.18—that is, a shaft with double circumferential grooves under torsion load (Fig. 1.18a), a semi-infinite element with double notches under tension (Fig. 1.18b), and an infinite element with circular and elliptical holes under tension (Fig. 1.18c)—an empirical formula (Nishida 1976)

$$K_{t1,2} \approx K_{t1c} + (K_{t2e} - K_{t1c}) \sqrt{1 - \frac{1}{4} \left(\frac{d}{b}\right)^2} \tag{1.22}$$

was developed. Under the loading conditions corresponding to Fig. 1.18a, b, and c, as appropriate, K_{t1c} is the stress concentration factor for an infinite element with a circular hole and K_{t2e} is the stress concentration factor for an element with the elliptical notch. This approximation is quite close to the theoretical solution of the cases of Fig. 1.18a and b. For the case of Fig. 1.18c, the error is somewhat larger, but the approximation is still adequate.

Another effective method is to use the *equivalent ellipse* concept. To illustrate the method, consider a flat element with a hexagonal hole (Fig. 1.19a). An ellipse of major semiaxes a and minimum radius of curvature r is the enveloping curve of two ends of the hexagonal hole. This ellipse is called the “equivalent ellipse” of the hexagonal hole. The stress concentration factor of a flat element with the equivalent elliptical hole (Fig. 1.19b) is (Eq. 4.58)

$$K_t = 2\sqrt{\frac{a}{r}} + 1 \tag{1.23}$$

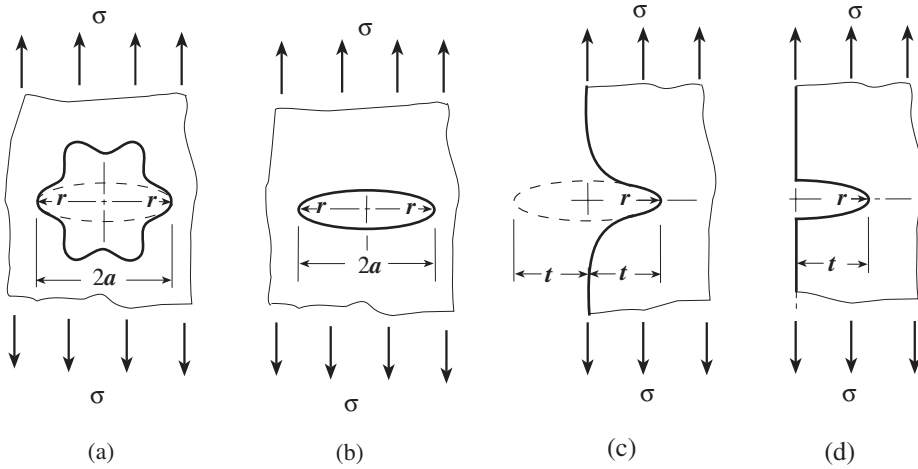


Figure 1.19 Equivalent ellipses: (a) element with a hexagonal hole; (b) element with an equivalent ellipse; (c) semi-infinite element with a groove; (d) semi-infinite element with the equivalent elliptical groove.

which is very close to the K_t for the flat element in Fig. 1.19a. Although this is an approximate method, the calculation is simple and the results are within an error of 10%. Similarly the stress concentration factor for a semi-infinite element with a groove under uniaxial tensile loading (Fig. 1.19c) can be estimated by finding K_t of the same element with the equivalent elliptical groove of Fig. 1.19d for which (Nishida 1976) (Eq. 4.58)

$$K_t = 2\sqrt{\frac{t}{r}} + 1 \tag{1.24}$$

1.8 THEORIES OF STRENGTH AND FAILURE

If our design problems involved only uniaxial stress problems, we would need to give only limited consideration to the problem of strength and failure of complex states of stress. However, even very simple load conditions may result in biaxial stress systems. An example is a thin spherical vessel subjected to internal pressure, resulting in biaxial tension acting on an element of the vessel. Another example is a bar of circular cross section subjected to tension, resulting in biaxial tension and compression acting at 45°.

From the standpoint of stress concentration cases, it should be noted that such simple loading as an axial tension produces biaxial surface stresses in a grooved bar (Fig. 1.20). Axial load P results in axial tension σ_1 and circumferential tension σ_2 acting on a surface element of the groove.

A considerable number of theories have been proposed relating uniaxial to biaxial or triaxial stress systems (Pilkey 2005); only the theories ordinarily utilized for design purposes are considered here. These are, for *brittle materials*,¹ the maximum stress criterion

¹The distinction between brittle and ductile materials is arbitrary, sometimes an elongation of 5% is considered to be the division between the two (Soderberg 1930).

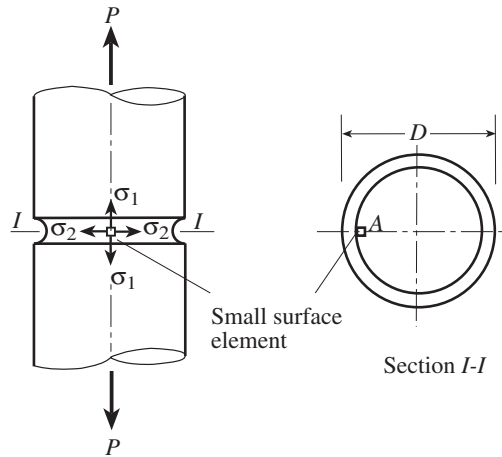


Figure 1.20 Biaxial stress in a notched tensile member.

and Mohr's theory and, for *ductile materials*, maximum shear theory and the von Mises criterion.

For the following theories it is assumed that the tension or compressive critical stresses (strength level, yield stress, or ultimate stress) are available. Also it is necessary to understand that any state of stress can be reduced through a rotation of coordinates to a state of stress involving only the principal stresses σ_1 , σ_2 , and σ_3 .

1.8.1 Maximum Stress Criterion

The *maximum stress criterion* (or *normal stress* or *Rankine criterion*) can be stated as follows: failure occurs in a multiaxial state of stress when either a principal tensile stress reaches the uniaxial tensile strength σ_{ut} or a principal compressive stress reaches the uniaxial compressive strength σ_{uc} . For a brittle material σ_{uc} is usually considerably greater than σ_{ut} . In Fig. 1.21, which represents biaxial conditions (σ_1 and σ_2 principal stresses, $\sigma_3 = 0$), the maximum stress criterion is represented by the square *CFHJ*.

The strength of a bar under uniaxial tension σ_{ut} is *OB* in Fig. 1.21. Note that according to the maximum stress criterion, the presence of an additional stress σ_2 at right angles does not affect the strength.

For torsion of a bar, only shear stresses appear on the cross section (i.e., $\sigma_x = \sigma_y = 0$, $\tau_{xy} = \tau$) and the principal stress (Pilkey 2005) $\sigma_2 = -\sigma_1 = \tau$ (line *AOE*). Since these principal stresses are equal in magnitude to the applied shear stress τ , the maximum stress condition of failure for torsion (*MA*, Fig. 1.21) is

$$\tau_u = \sigma_{ut} \quad (1.25)$$

In other words, according to the maximum stress criterion, the torsion and tension strength values should be equal.

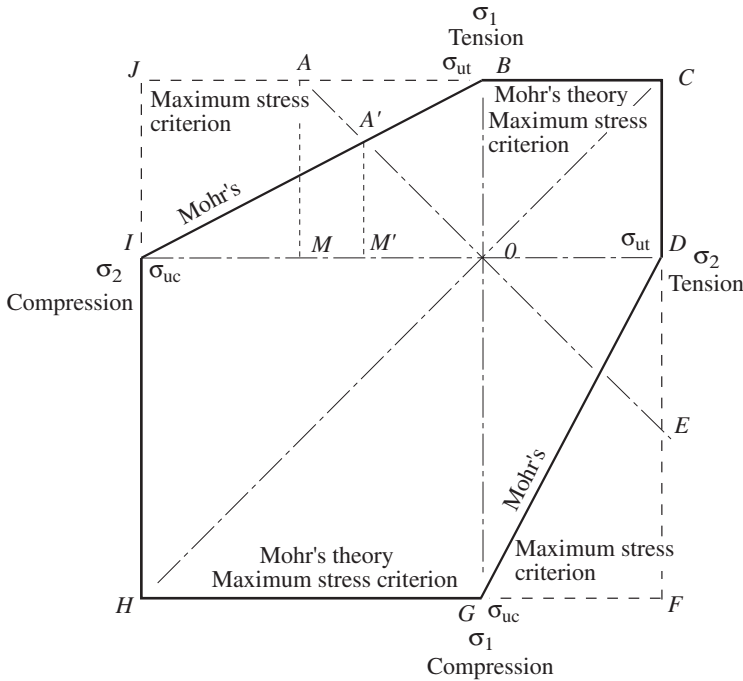


Figure 1.21 Biaxial conditions for strength theories for brittle materials.

1.8.2 Mohr's Theory

The condition of failure of brittle materials according to *Mohr's theory* (or the *Coulomb-Mohr theory* or *internal friction theory*) is illustrated in Fig. 1.22. Circles of diameters σ_{ut} and σ_{uc} are drawn as shown. A stress state, for which the Mohr's circle just contacts the line of tangency² of the σ_{ut} and σ_{uc} circles, represents a condition of failure (Pilkey 2005). See the Mohr's circle (dashed) of diameter $\sigma_1 - \sigma_2$ of Fig. 1.22. The resultant plot for biaxial conditions is shown in Fig. 1.21. The conditions of failure are as follows:

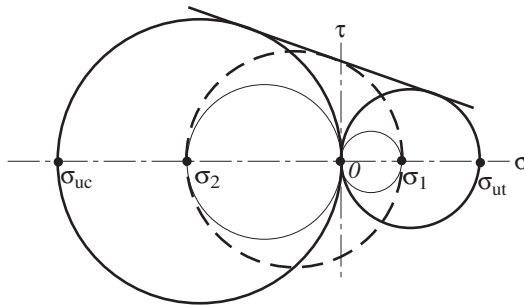


Figure 1.22 Mohr's theory of failure of brittle materials.

²The straight line is a special case of the more general Mohr's theory, which is based on a curved envelope.

For $\sigma_1 \geq 0$ and $\sigma_2 \geq 0$ (first quadrant), with $\sigma_1 \geq \sigma_2$

$$\sigma_1 = \sigma_{ut} \tag{1.26}$$

For $\sigma_1 \geq 0$ and $\sigma_2 \leq 0$ (second quadrant)

$$\frac{\sigma_1}{\sigma_{ut}} - \frac{\sigma_2}{\sigma_{uc}} = 1 \tag{1.27}$$

For $\sigma_1 \leq 0$ and $\sigma_2 \leq 0$ (third quadrant)

$$\sigma_2 = -\sigma_{uc} \tag{1.28}$$

For $\sigma_1 \leq 0$ and $\sigma_2 \geq 0$ (fourth quadrant)

$$-\frac{\sigma_1}{\sigma_{uc}} + \frac{\sigma_2}{\sigma_{ut}} = 1 \tag{1.29}$$

As will be seen later (Fig. 1.23) this is similar to the representation for the maximum shear theory, except for nonsymmetry.

Certain tests of brittle materials seem to substantiate the maximum stress criterion (Draffin and Collins 1938), whereas other tests and reasoning lead to a preference for Mohr's theory (Marin 1952). The maximum stress criterion gives the same results in the first and third quadrants. For the torsion case ($\sigma_2 = -\sigma_1$), use of Mohr's theory is on the "safe side," since the limiting strength value used is $M'A'$ instead of MA (Fig. 1.21). The following can be shown for $M'A'$ of Fig. 1.21:

$$\tau_u = \frac{\sigma_{ut}}{1 + (\sigma_{ut}/\sigma_{uc})} \tag{1.30}$$

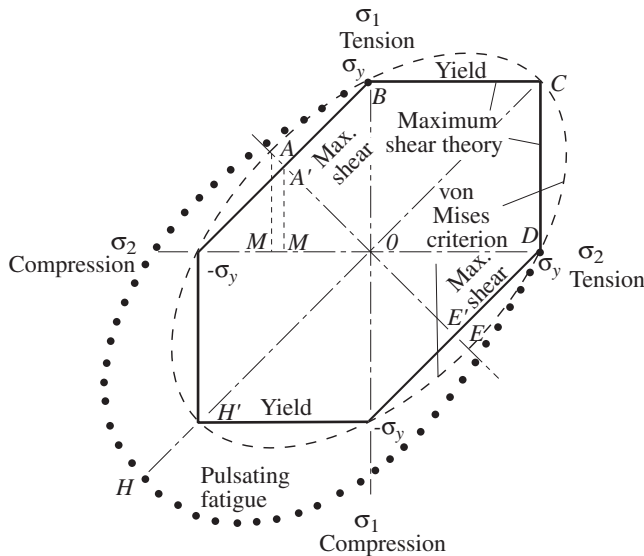


Figure 1.23 Biaxial conditions for strength theories for ductile materials.

1.8.3 Maximum Shear Theory

The *maximum shear theory* (or *Tresca's* or *Guest's theory*) was developed as a criterion for yield or failure, but it has also been applied to fatigue failure, which in ductile materials is thought to be initiated by the maximum shear stress (Gough 1933). According to the maximum shear theory, failure occurs when the maximum shear stress in a multiaxial system reaches the value of the shear stress in a uniaxial bar at failure. In Fig. 1.23, the maximum shear theory is represented by the six-sided figure. For principal stresses σ_1 , σ_2 , and σ_3 , the maximum shear stresses are (Pilkey 2005)

$$\frac{\sigma_1 - \sigma_2}{2}, \quad \frac{\sigma_1 - \sigma_3}{2}, \quad \frac{\sigma_2 - \sigma_3}{2} \quad (1.31)$$

The actual maximum shear stress is the peak value of the expressions of Eq. (1.31). The value of the shear failure stress in a simple tensile test is $\sigma/2$, where σ is the tensile failure stress (yield σ_y or fatigue σ_f) in the tensile test. Suppose that fatigue failure is of interest and that σ_f is the uniaxial fatigue limit in alternating tension and compression. For the biaxial case set $\sigma_3 = 0$, and suppose that σ_1 is greater than σ_2 for both in tension. Then failure occurs when $(\sigma_1 - 0)/2 = \sigma_f/2$ or $\sigma_1 = \sigma_f$. This is the condition represented in the first quadrant of Fig. 1.23 where σ_y rather than σ_f is displayed. However, in the second and fourth quadrants, where the biaxial stresses are of opposite sign, the situation is different. For $\sigma_2 = -\sigma_1$, represented by line AE of Fig. 1.23, failure occurs in accordance with the maximum shear theory when $[\sigma_1 - (-\sigma_1)]/2 = \sigma_f/2$ or $\sigma_1 = \sigma_f/2$, namely $M'A' = OB/2$ in Fig. 1.23.

In the torsion test $\sigma_2 = -\sigma_1 = \tau$,

$$\tau_f = \frac{\sigma_f}{2} \quad (1.32)$$

This is half the value corresponding to the maximum stress criterion.

1.8.4 von Mises Criterion

The following expression was proposed by R. von Mises (1913), as representing a criterion of failure by yielding:

$$\sigma_y = \sqrt{\frac{(\sigma_1 - \sigma_2)^2 + (\sigma_2 - \sigma_3)^2 + (\sigma_1 - \sigma_3)^2}{2}} \quad (1.33)$$

where σ_y is the yield strength in a uniaxially loaded bar. For another failure mode, such as fatigue failure, replace σ_y by the appropriate stress level, such as σ_f . The quantity on the right-hand side of Eq. (1.33), which is sometimes available as output of structural analysis software, is often referred to as the *equivalent stress* σ_{eq} :

$$\sigma_{eq} = \sqrt{\frac{(\sigma_1 - \sigma_2)^2 + (\sigma_2 - \sigma_3)^2 + (\sigma_1 - \sigma_3)^2}{2}} \quad (1.34)$$

This theory, which is also called the *Maxwell-Huber-Hencky-von Mises theory*, *octahedral shear stress theory* (Eichinger 1926; Nadai 1937), and *maximum distortion energy theory* (Hencky 1924), states that failure occurs when the energy of distortion reaches the same

energy for failure in tension.³ If $\sigma_3 = 0$, Eq. (1.34) reduces to

$$\sigma_{\text{eq}} = \sqrt{\sigma_1^2 - \sigma_1\sigma_2 + \sigma_2^2} \quad (1.35)$$

This relationship is shown by the dashed ellipse of Fig. 1.23 with $OB = \sigma_y$. Unlike the six-sided figure, it does not have the discontinuities in slope, which seem unrealistic in a physical sense. Sachs (1928) and Cox and Sopwith (1937) maintain that close agreement with the results predicted by Eq. (1.33) is obtained if one considers the statistical behavior of a randomly oriented aggregate of crystals.

For the torsion case with $\sigma_2 = -\sigma_1 = \tau_y$, the von Mises criterion becomes

$$\tau_y = \frac{\sigma_y}{\sqrt{3}} = 0.577\sigma_y \quad (1.36)$$

or $MA = (0.577)OB$ in Fig. 1.23, where τ_y is the yield strength of a bar in torsion. Note from Figs. 1.21 and 1.23 that all the foregoing theories are in agreement at C , representing equal tensions, but they differ along AE , representing tension and compression of equal magnitudes (torsion).

Yield tests of ductile materials have shown that the von Mises criterion interprets well the results of a variety of biaxial conditions. It has been pointed out (Prager and Hodge 1951) that although the agreement must be regarded as fortuitous, the von Mises criterion would still be of practical interest because of its mathematical simplicity even if the agreement with test results had been less satisfactory.

There is evidence (Nisihara and Kojima 1939; Peterson 1974) that for ductile materials the von Mises criterion also gives a reasonably good interpretation of fatigue results in the upper half ($ABCDE$) of the ellipse of Fig. 1.23 for completely alternating or pulsating tension cycling. As shown in Fig. 1.24, results from alternating tests are in better agreement with the von Mises criterion (upper line) than with the maximum shear theory (lower line). If yielding is considered the criterion of failure, the ellipse of Fig. 1.23 is symmetrical about AE . With regard to the region below AE (compression side), there is evidence that for pulsating compression (e.g., 0 to maximum compression) this area is considerably enlarged (Nisihara and Kojima 1939; Rôds and Eichinger 1950; Newmark et al. 1951). For the cases treated here we deal primarily with the upper area.⁴

1.8.5 Observations on the Use of the Theories of Failure

If a member is in a uniaxial stress state (i.e., $\sigma_{\text{max}} = \sigma_1$, $\sigma_2 = \sigma_3 = 0$), the maximum stress can be used directly in $\sigma_{\text{max}} = K_t\sigma_{\text{nom}}$ for a failure analysis. However, when the location of the maximum stress is in a biaxial or triaxial stress state, it is important to consider not only the effects of σ_1 but also of σ_2 and σ_3 , according to one of the theories

³The proposals of both von Mises and Hencky were to a considerable extent anticipated by Huber in 1904. Although limited to mean compression and without specifying mode of failure; his paper in the Polish language did not attract international attention until 20 years later.

⁴It will be noted that all representations in Figs. 1.21 and 1.23 are symmetrical about line HC . In some cases, such as forgings and bars, strong directional effects can exist (i.e., transverse strength can be considerably less than longitudinal strength). Findley (1951) gives methods for taking anisotropy into account in applying strength theories.

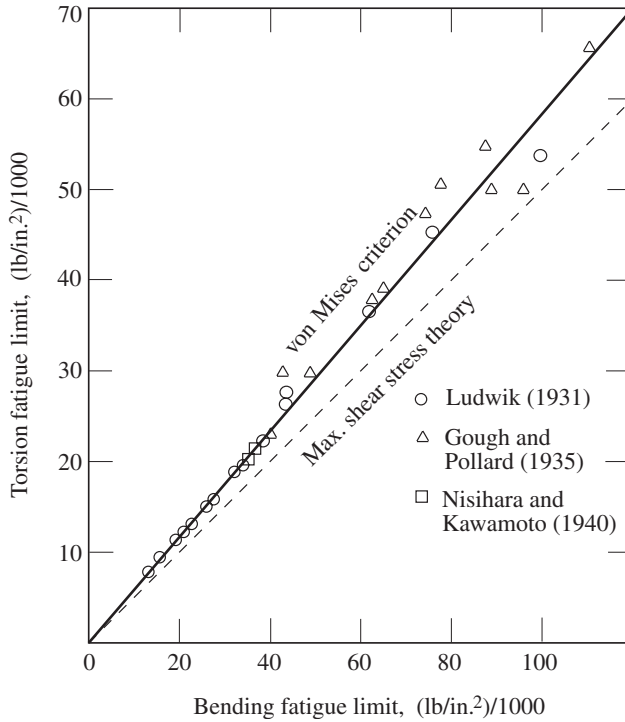


Figure 1.24 Comparison of torsion and bending fatigue limits for ductile materials.

of strength (failure). For example, for a shaft with a circumferential groove under tensile loading, a point at the bottom of the groove is in a biaxial stress state; that is, the point is subjected to axial stress σ_1 and circumferential stress σ_2 as shown in Fig. 1.20. If the von Mises theory is used in a failure analysis, then (Eq. 1.35)

$$\sigma_{eq} = \sqrt{\sigma_1^2 - \sigma_1\sigma_2 + \sigma_2^2} \tag{1.37}$$

To combine the stress concentration and the von Mises strength theory, introduce a factor K'_t :

$$K'_t = \frac{\sigma_{eq}}{\sigma} \tag{1.38}$$

where $\sigma = 4P/(\pi D^2)$ is the reference stress. Substitute Eq. (1.37) into Eq. (1.38),

$$K'_t = \frac{\sigma_1}{\sigma} \sqrt{1 - \frac{\sigma_2}{\sigma_1} + \left(\frac{\sigma_2}{\sigma_1}\right)^2} = K_t \sqrt{1 - \frac{\sigma_2}{\sigma_1} + \left(\frac{\sigma_2}{\sigma_1}\right)^2} \tag{1.39}$$

where $K_t = \sigma_1/\sigma$ is defined as the stress concentration factor at point A that can be read from a chart of this book. Usually, $0 < \sigma_2/\sigma_1 < 1$, so that $K'_t < K_t$. In general, K'_t is about 90% to 95% of the value of K_t and not less than 85%.

Consider the case of a three-dimensional block with a spherical cavity under uniaxial tension σ . The two principal stresses at point A on the surface of the cavity (Fig. 1.25) are

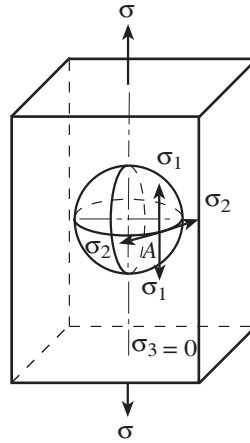


Figure 1.25 Block with a spherical cavity.

(Nishida 1976)

$$\sigma_1 = \frac{3(9 - 5\nu)}{2(7 - 5\nu)}\sigma, \quad \sigma_2 = \frac{3(5\nu - 1)}{2(7 - 5\nu)}\sigma \quad (1.40)$$

From these relationships

$$\frac{\sigma_2}{\sigma_1} = \frac{5\nu - 1}{9 - 5\nu} \quad (1.41)$$

Substitute Eq. (1.41) into Eq. (1.39):

$$K'_t = K_t \sqrt{1 - \frac{5\nu - 1}{9 - 5\nu} + \left(\frac{5\nu - 1}{9 - 5\nu}\right)^2} \quad (1.42)$$

For $\nu = 0.4$,

$$K'_t = 0.94K_t$$

and when $\nu = 0.3$,

$$K'_t = 0.97K_t$$

It is apparent that K'_t is lower than and quite close to K_t . It can be concluded that the usual design using K_t is on the safe side and will not be accompanied by significant errors. Therefore charts for K'_t are not included in this book.

1.8.6 Stress Concentration Factors under Combined Loads: Principle of Superposition

In practice, a structural member is often under the action of several types of loads, instead of being subjected to a single type of loading as represented in the graphs of this book. In such

a case, evaluate the stress for each type of load separately, and superimpose the individual stresses. Since superposition presupposes a linear relationship between the applied loading and resulting response, it is necessary that the maximum stress be less than the elastic limit of the material. The following examples illustrate this procedure.

Example 1.5 Tension and Bending of a Two-Dimensional Element A notched thin element is under combined loads of tension and in-plane bending as shown in Fig. 1.26. Find the maximum stress.

For tension load P , the stress concentration factor K_{t1} can be found from Chart 2.3 and the maximum stress is

$$\sigma_{\max 1} = K_{t1} \sigma_{\text{nom}1} \quad (1)$$

in which $\sigma_{\text{nom}1} = P/(dh)$. For the in-plane bending moment M , the maximum bending stress is (the stress concentration factor can be found from Chart 2.25)

$$\sigma_{\max 2} = K_{t2} \sigma_{\text{nom}2} \quad (2)$$

where $\sigma_{\text{nom}2} = 6M/(d^2h)$ is the stress at the base of the groove. Stresses $\sigma_{\max 1}$ and $\sigma_{\max 2}$ are both normal stresses that occur at the same point, namely at the base of the groove. Hence, when the element is under these combined loads, the maximum stress at the notch is

$$\sigma_{\max} = \sigma_{\max 1} + \sigma_{\max 2} = K_{t1} \sigma_{\text{nom}1} + K_{t2} \sigma_{\text{nom}2} \quad (3)$$

Example 1.6 Tension, Bending, and Torsion of a Grooved Shaft A shaft of circular cross section with a circumferential groove is under the combined loads of axial force P , bending moment M , and torque T , as shown in Fig. 1.27. Calculate the maximum stresses corresponding to the various failure theories.

The maximum stress is (the stress concentration factor of this shaft due to axial force P can be found from Chart 2.19)

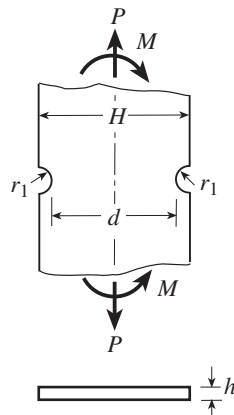


Figure 1.26 Element under tension and bending loading.

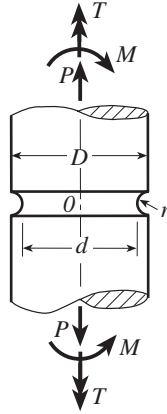


Figure 1.27 Grooved shaft subject to tension, bending, and torsion.

$$\sigma_{\max 1} = K_{m1} \frac{4P}{\pi d^2} \quad (1)$$

The maximum stress corresponding to the bending moment (from Chart 2.41) is

$$\sigma_{\max 2} = K_{m2} \frac{32M}{\pi d^3} \quad (2)$$

The maximum torsion stress due to torque T is obtained from Chart 2.47 as

$$\tau_{\max 3} = K_{ts} \frac{16T}{\pi d^3} \quad (3)$$

The maximum stresses of Eqs. (1)–(3) occur at the same location, namely at the base of the groove, and the principal stresses are calculated using the familiar formulas (Pilkey 2005)

$$\sigma_1 = \frac{1}{2}(\sigma_{\max 1} + \sigma_{\max 2}) + \frac{1}{2}\sqrt{(\sigma_{\max 1} + \sigma_{\max 2})^2 + 4\tau_{\max 3}^2} \quad (4)$$

$$\sigma_2 = \frac{1}{2}(\sigma_{\max 1} + \sigma_{\max 2}) - \frac{1}{2}\sqrt{(\sigma_{\max 1} + \sigma_{\max 2})^2 + 4\tau_{\max 3}^2} \quad (5)$$

The various failure criteria for the base of the groove can now be formulated.

Maximum Stress Criterion

$$\sigma_{\max} = \sigma_1 \quad (6)$$

Mohr's Theory From Eqs. (4) and (5), it is easy to prove that $\sigma_1 > 0$ and $\sigma_2 < 0$. The condition of failure is (Eq. 1.27)

$$\frac{\sigma_1}{\sigma_{ut}} - \frac{\sigma_2}{\sigma_{uc}} = 1 \quad (7)$$

where σ_{ut} is the uniaxial tensile strength and σ_{uc} is the uniaxial compressive strength.

Maximum Shear Theory Since $\sigma_1 > 0$, $\sigma_2 < 0$, $\sigma_3 = 0$, the maximum shear stress is

$$\tau_{\max} = \frac{\sigma_1 - \sigma_2}{2} = \frac{1}{2} \sqrt{(\sigma_{\max 1} + \sigma_{\max 2})^2 + 4\tau_{\max 3}^2} \quad (8)$$

von Mises Criterion From Eq. (1.34),

$$\sigma_{\text{eq}} = \sqrt{\sigma_1^2 - \sigma_1\sigma_2 + \sigma_2^2} = \sqrt{(\sigma_{\max 1} + \sigma_{\max 2})^2 + 3\tau_{\max 3}^2} \quad (9)$$

Example 1.7 Infinite Element with a Circular Hole with Internal Pressure Find the stress concentration factor for an infinite element subjected to internal pressure p on its circular hole edge as shown in Fig. 1.28a.

This example can be solved by superimposing two configurations. The loads on the element can be assumed to consist of two cases: (1) biaxial tension $\sigma = p$ (Fig. 1.28b); (2) biaxial compression $\sigma = -p$, with pressure on the circular hole edge (Fig. 1.28c).

For case 1, $\sigma = p$, the stresses at the edge of the hole are (Eq. 4.16)

$$\begin{aligned} \sigma_{r1} &= 0 \\ \sigma_{\theta 1} &= 2p \\ \tau_{r\theta 1} &= 0 \end{aligned} \quad (1)$$

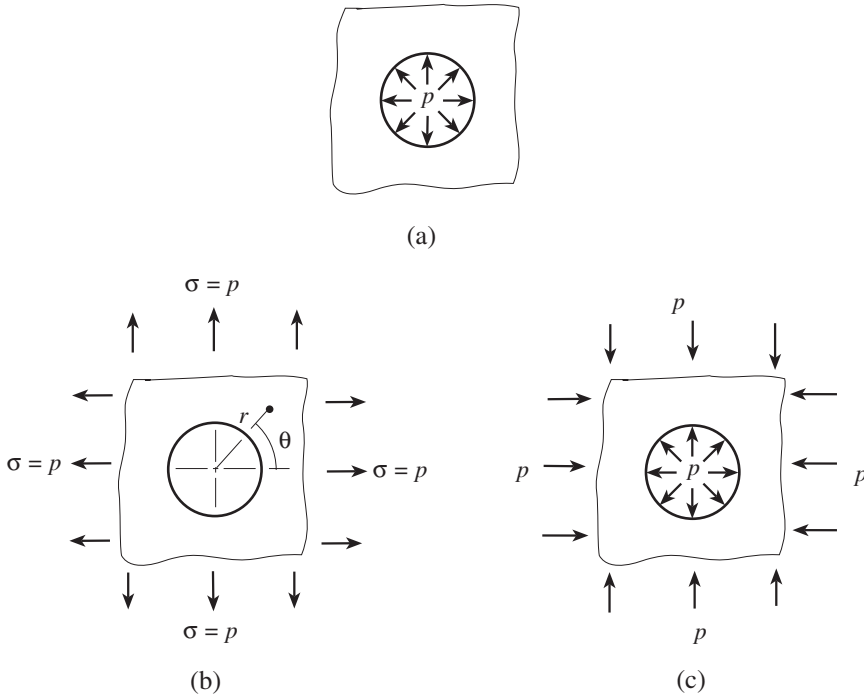


Figure 1.28 (a) Infinite element subjected to internal pressure p on a circular hole edge; (b) element under biaxial tension at area remote from the hole; (c) element under biaxial compression.

For case 2 the stresses at the edge of the hole (hydrostatic pressure) are

$$\begin{aligned}\sigma_{r2} &= -p \\ \sigma_{\theta2} &= -p \\ \tau_{r\theta2} &= 0\end{aligned}\quad (2)$$

The stresses for both cases can be derived from the formulas of Little (1973). The total stresses at the edge of the hole can be obtained by superposition

$$\begin{aligned}\sigma_r &= \sigma_{r1} + \sigma_{r2} = -p \\ \sigma_\theta &= \sigma_{\theta1} + \sigma_{\theta2} = p \\ \tau_{r\theta} &= \tau_{r\theta1} + \tau_{r\theta2} = 0\end{aligned}\quad (3)$$

The maximum stress is $\sigma_{\max} = p$. If p is taken as the nominal stress (Example 1.3), the corresponding stress concentration factor can be defined as

$$K_t = \frac{\sigma_{\max}}{\sigma_{\text{nom}}} = \frac{\sigma_{\max}}{p} = 1 \quad (4)$$

1.9 NOTCH SENSITIVITY

As noted at the beginning of this chapter, the theoretical stress concentration factors apply mainly to ideal elastic materials and depend on the geometry of the body and the loading. Sometimes a more realistic model is preferable. When the applied loads reach a certain level, plastic deformations may be involved. The actual strength of structural members may be quite different from that derived using theoretical stress concentration factors, especially for the cases of impact and alternating loads.

It is reasonable to introduce the concept of the *effective stress concentration factor* K_e . This is also referred to as the factor of stress concentration at rupture or the notch rupture strength ratio (ASTM 1994). The magnitude of K_e is obtained experimentally. For instance, K_e for a round bar with a circumferential groove subjected to a tensile load P' (Fig. 1.29a) is obtained as follows: (1) Prepare two sets of specimens of the actual material, the round bars of the first set having circumferential grooves, with d as the diameter at the root of the groove (Fig. 1.29a). The round bars of the second set are of diameter d without grooves (Fig. 1.29b). (2) Perform a tensile test for the two sets of specimens, the rupture load for the first set is P' , while the rupture load for second set is P . (3) The effective stress concentration factor is defined as

$$K_e = \frac{P}{P'} \quad (1.43)$$

In general, $P' < P$ so that $K_e > 1$. The effective stress concentration factor is a function not only of geometry but also of material properties. Some characteristics of K_e for static loading of different materials are discussed briefly below.

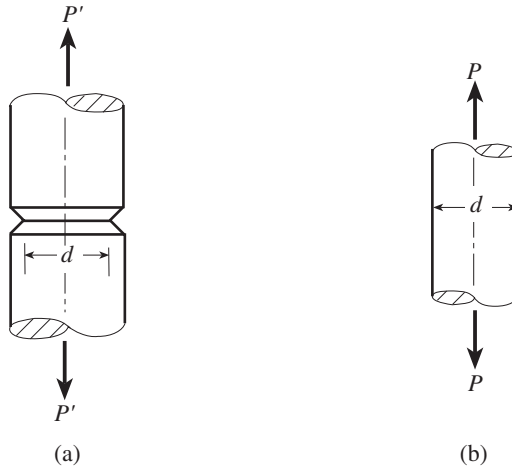


Figure 1.29 Specimens for obtaining K_t .

1. *Ductile material.* Consider a tensile loaded plane element with a V-shaped notch. The material law for the material is sketched in Fig. 1.30. If the maximum stress at the root of the notch is less than the yield strength $\sigma_{max} < \sigma_y$, the stress distributions near the notch would appear as in curves 1 and 2 in Fig. 1.30. The maximum stress value is

$$\sigma_{max} = K_t \sigma_{nom} \tag{1.44}$$

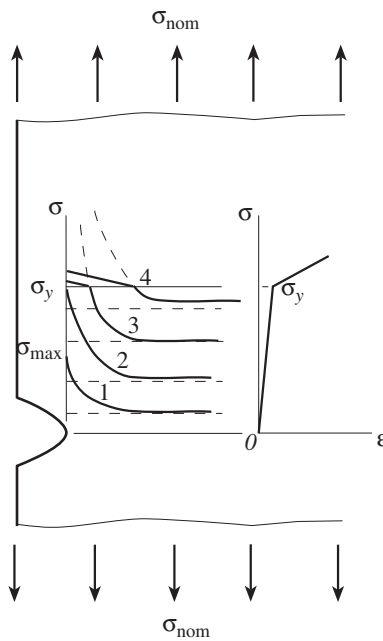


Figure 1.30 Stress distribution near a notch for a ductile material.

As the σ_{\max} exceeds σ_y , the strain at the root of the notch continues to increase but the maximum stress increases only slightly. The stress distributions on the cross section will be of the form of curves 3 and 4 in Fig. 1.30. Equation (1.44) no longer applies to this case. As σ_{nom} continues to increase, the stress distribution at the notch becomes more uniform and the effective stress concentration factor K_e is close to unity.

2. *Brittle material.* Most brittle materials can be treated as elastic bodies. When the applied load increases, the stress and strain retain their linear relationship until damage occurs. The effective stress concentration factor K_e is the same as K_t .
3. *Gray cast iron.* Although gray cast irons belong to brittle materials, they contain flake graphite dispersed in the steel matrix and a number of small cavities, which produce much higher stress concentrations than would be expected from the geometry of the discontinuity. In such a case the use of the stress concentration factor K_t may result in significant error and K_e can be expected to approach unity, since the stress raiser has a smaller influence on the strength of the member than that of the small cavities and flake graphite.

It can be reasoned from these three cases that the effective stress concentration factor depends on the characteristics of the material and the nature of the load, as well as the geometry of the stress raiser. Also $1 \leq K_e \leq K_t$. The maximum stress at rupture can be defined to be

$$\sigma_{\max} = K_e \sigma_{\text{nom}} \quad (1.45)$$

To express the relationship between K_e and K_t , introduce the concept of *notch sensitivity* q (Boresi et al. 1993):

$$q = \frac{K_e - 1}{K_t - 1} \quad (1.46)$$

or

$$K_e = q(K_t - 1) + 1 \quad (1.47)$$

Substitute Eq. (1.47) into Eq. (1.45):

$$\sigma_{\max} = [q(K_t - 1) + 1] \sigma_{\text{nom}} \quad (1.48)$$

If $q = 0$, then $K_e = 1$, meaning that the stress concentration does not influence the strength of the structural member. If $q = 1$, then $K_e = K_t$, implying that the theoretical stress concentration factor should be fully invoked. The notch sensitivity is a measure of the agreement between K_e and K_t .

The concepts of the effective stress concentration factor and notch sensitivity are used primarily for fatigue strength design. For fatigue loading, replace K_e in Eq. (1.43) by K_f or K_{fs} , defined as

$$K_f = \frac{\text{Fatigue limit of unnotched specimen (axial or bending)}}{\text{Fatigue limit of notched specimen (axial or bending)}} = \frac{\sigma_f}{\sigma_{nf}} \quad (1.49)$$

$$K_{fs} = \frac{\text{Fatigue limit of unnotched specimen (shear stress)}}{\text{Fatigue limit of notched specimen (shear stress)}} = \frac{\tau_f}{\tau_{nf}} \quad (1.50)$$

where K_f is the *fatigue notch factor* for normal stress and K_{fs} is the fatigue notch factor for shear stress, such as torsion. The notch sensitivities for fatigue become

$$q = \frac{K_f - 1}{K_t - 1} \quad (1.51)$$

or

$$q = \frac{K_{fs} - 1}{K_{ts} - 1} \quad (1.52)$$

where K_{ts} is defined in Eq. (1.2). The values of q vary from $q = 0$ for no notch effect ($K_f = 1$) to $q = 1$ for the full theoretical effect ($K_f = K_t$).

Equations (1.51) and (1.52) can be rewritten in the following form for design use:

$$K_{tf} = q(K_t - 1) + 1 \quad (1.53)$$

$$K_{tsf} = q(K_{ts} - 1) + 1 \quad (1.54)$$

where K_{tf} is the *estimated* fatigue notch factor for normal stress, a calculated factor using an average q value obtained from Fig. 1.31 or a similar curve, and K_{tsf} is the *estimated* fatigue notch factor for shear stress.

If no information on q is available, as would be the case for newly developed materials, it is suggested that the full theoretical factor, K_t or K_{ts} , be used. It should be noted in this

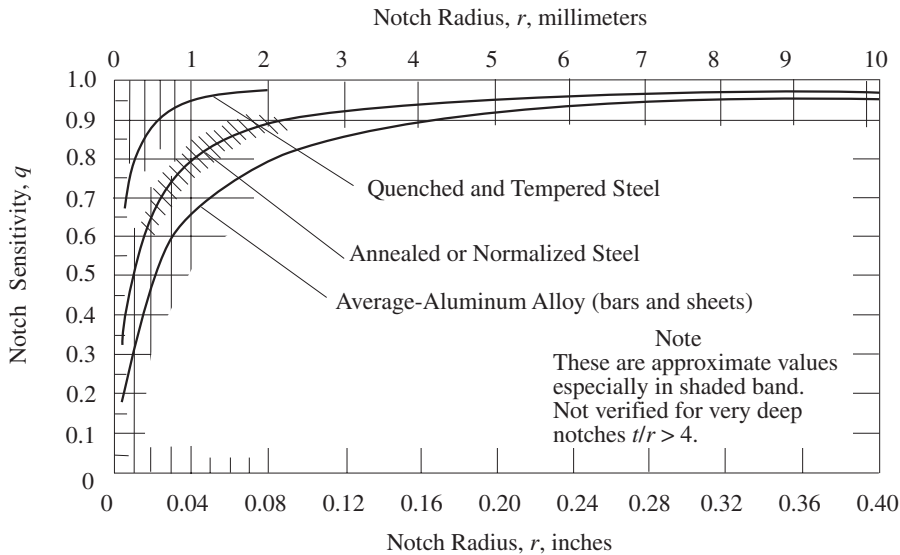


Figure 1.31 Average fatigue notch sensitivity.

connection that if notch sensitivity is not taken into consideration at all in design ($q = 1$), the error will be on the safe side ($K_{t_f} = K_t$ in Eq. (1.53)).

In plotting K_f for geometrically similar specimens, it was found that typically K_f decreased as the specimen size decreased (Peterson 1933a,b, 1943; Peterson and Wahl 1936). For this reason it is not possible to obtain reliable comparative q values for different materials by making tests of a standardized specimen of fixed dimension (Peterson 1945). Since the local stress distribution (stress gradient,⁵ volume at peak stress) is more dependent on the notch radius r than on other geometrical variables (Peterson 1938; von Phillip 1942; Neuber 1958), it was apparent that it would be more logical to plot q versus r rather than q versus d (for geometrically similar specimens the curve shapes are of course the same). Plotted q versus r curves (Peterson 1950, 1959) based on available data (Gunn 1952; Lazan and Blatherwick 1953; Templin 1954; Fralich 1959) were found to be within reasonable scatter bands.

A q versus r chart for design purposes is given in Fig. 1.31; it averages the previously mentioned plots. Note that the chart is not verified for notches having a depth greater than four times the notch radius because data are not available. Also note that the curves are to be considered as approximate (see shaded band).

Notch sensitivity values for radii approaching zero still must be studied. It is, however, well known that tiny holes and scratches do not result in a strength reduction corresponding to theoretical stress concentration factors. In fact, in steels of low tensile strength, the effect of very small holes or scratches is often quite small. However, in higher-strength steels the effect of tiny holes or scratches is more pronounced. Much more data are needed, preferably obtained from statistically planned investigations. Until better information is available, Fig. 1.31 provides reasonable values for design use.

Several expressions have been proposed for the q versus r curve. Such a formula could be useful in setting up a computer design program. Since it would be unrealistic to expect failure at a volume corresponding to the point of peak stress because of the plastic deformation (Peterson 1938), formulations for K_f are based on failure over a distance below the surface (Neuber 1958; Peterson 1974). From the K_f formulations, q versus r relations are obtained. These and other variations are found in the literature (Peterson 1945). All of the formulas yield acceptable results for design purposes. One must, however, always remember the approximate nature of the relations. In Fig. 1.31 the following simple formula (Peterson 1959) is used⁶:

$$q = \frac{1}{1 + \alpha/r} \quad (1.55)$$

where α is a material constant and r is the notch radius.

In Fig. 1.31, $\alpha = 0.0025$ for quenched and tempered steel, $\alpha = 0.01$ for annealed or normalized steel, $\alpha = 0.02$ for aluminum alloy sheets and bars (avg.). In Peterson (1959) more detailed values are given, including the following approximate design values for steels as a function of tensile strength:

⁵The stress is approximately linear in the peak stress region (Peterson 1938; Leven 1955).

⁶The corresponding Kuhn-Hardrath formula (Kuhn and Hardrath 1952) based on Neuber relations is

$$q = \frac{1}{1 + \sqrt{\rho'/r}}$$

Either formula may be used for design purposes (Peterson 1959). The quantities α or ρ' , a material constant, are determined by test data.

$\sigma_{ut}/1000$	α
50	0.015
75	0.010
100	0.007
125	0.005
150	0.0035
200	0.0020
250	0.0013

where σ_{ut} = tensile strength in pounds per square inch. In using the foregoing α values, one must keep in mind that the curves represent averages (see shaded band in Fig. 1.31).

A method has been proposed by Neuber (1968) wherein an equivalent larger radius is used to provide a lower K factor. The increment to the radius is dependent on the stress state, the kind of material, and its tensile strength. Application of this method gives results that are in reasonably good agreement with the calculations of other methods (Peterson 1953).

1.10 DESIGN RELATIONS FOR STATIC STRESS

1.10.1 Ductile Materials

As discussed in Section 1.8, under ordinary conditions a ductile member loaded with a steadily increasing uniaxial stress does not suffer loss of strength due to the presence of a notch, since the notch sensitivity q usually lies in the range 0 to 0.1. However, if the function of the member is such that the amount of inelastic strain required for the strength to be insensitive to the notch is restricted, the value of q may approach 1.0 ($K_e = K_t$). If the member is loaded statically and is also subjected to shock loading, or if the part is to be subjected to high (Davis and Manjoine 1952) or low temperature, or if the part contains sharp discontinuities, a ductile material may behave in the manner of a brittle material, which should be studied with fracture mechanics methods. These are special cases. If there is doubt, K_t should be applied ($q = 1$). Ordinarily, for static loading of a ductile material, set $q = 0$ in Eq. (1.48), namely $\sigma_{\max} = \sigma_{\text{nom}}$.⁷

Traditionally, design safety is measured by the *factor of safety* n . It is defined as the ratio of the load that would cause failure of the member to the working stress on the member. For ductile material the failure is assumed to be caused by yielding and the equivalent stress σ_{eq} can be used as the working stress (von Mises criterion of failure, Section 1.8). For axial loading (normal, or direct, stress $\sigma_1 = \sigma_{0d}$, $\sigma_2 = \sigma_3 = 0$):

$$n = \frac{\sigma_y}{\sigma_{0d}} \quad (1.56)$$

⁷This consideration is on the basis of strength only. Stress concentration does not ordinarily reduce the strength of a notched member in a static test, but usually it does reduce total deformation to rupture. This means lower "ductility," or, expressed in a different way, less area under the stress-strain diagram (less energy expended in producing complete failure). It is often of major importance to have as much energy-absorption capacity as possible (cf. metal versus plastic for an automobile body). However, this is a consideration depending on consequence of failure, and so on, and is not within the scope of this book, which deals only with strength factors. Plastic behavior is involved in a limited way in the use of the factor L , as is discussed in this section.

where σ_y is the yield strength and σ_{0d} is the static normal stress = $\sigma_{eq} = \sigma_1$. For bending ($\sigma_1 = \sigma_{0b}$, $\sigma_2 = \sigma_3 = 0$),

$$n = \frac{L_b \sigma_y}{\sigma_{0b}} \quad (1.57)$$

where L_b is the limit design factor for bending and σ_{0b} is the static bending stress.

In general, the limit design factor L is the ratio of the load (force or moment) needed to cause complete yielding throughout the section of a bar to the load needed to cause initial yielding at the "extreme fiber" (Van den Broek 1942), assuming no stress concentration. For tension, $L = 1$; for bending of a rectangular bar, $L_b = 3/2$; for bending of a round bar, $L_b = 16/(3\pi) = 1.70$; for torsion of a round bar, $L_s = 4/3$; for a tube, it can be shown that for bending and torsion, respectively,

$$L_b = \frac{16}{3\pi} \left[\frac{1 - (d_i/d_0)^3}{1 - (d_i/d_0)^4} \right] \quad (1.58)$$

$$L_s = \frac{4}{3} \left[\frac{1 - (d_i/d_0)^3}{1 - (d_i/d_0)^4} \right]$$

where d_i and d_0 are the inside and outside diameters, respectively, of the tube. These relations are plotted in Fig. 1.32.

Criteria other than complete yielding can be used. For a rectangular bar in bending, L_b values have been calculated (Steele et al. 1952), yielding to 1/4 depth $L_b = 1.22$, and yielding to 1/2 depth $L_b = 1.375$; for 0.1% inelastic strain in steel with yield point of 30,000 psi, $L_b = 1.375$. For a circular bar in bending, yielding to 1/4 depth, $L_b = 1.25$, and yielding to 1/2 depth, $L_b = 1.5$. For a tube $d_i/d_0 = 3/4$: yielding 1/4 depth, $L_b = 1.23$, and yielding 1/2 depth, $L_b = 1.34$.

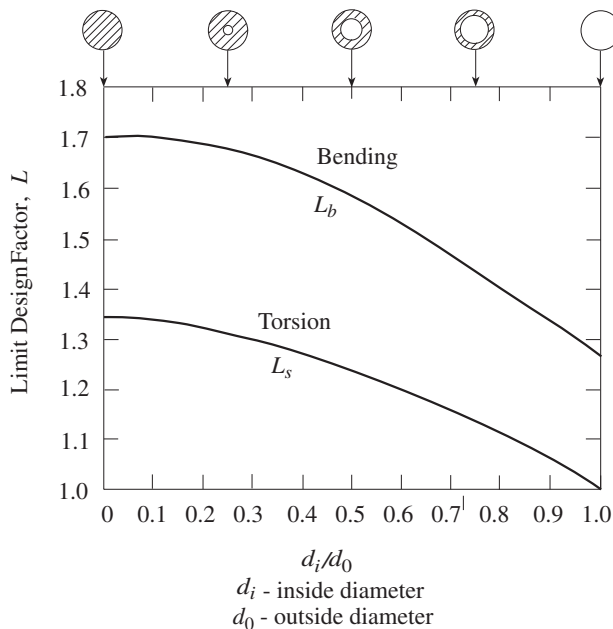


Figure 1.32 Limit design factors for tubular members.

All the foregoing L values are based on the assumption that the stress-strain diagram becomes horizontal after the yield point is reached, that is, the material is *elastic, perfectly plastic*. This is a reasonable assumption for low- or medium-carbon steel. For other stress-strain diagrams which can be represented by a sloping line or curve beyond the elastic range, a value of L closer to 1.0 should be used (Van den Broek 1942). For design $L\sigma_y$ should not exceed the tensile strength σ_{ut} .

For torsion of a round bar (shear stress), using Eq. (1.36) obtains

$$n = \frac{L_s \tau_y}{\tau_0} = \frac{L_s \sigma_y}{\sqrt{3} \tau_0} \quad (1.59)$$

where τ_y is the yield strength in torsion and τ_0 is the static shear stress.

For combined normal (axial and bending) and shear stress the principal stresses are

$$\begin{aligned} \sigma_1 &= \frac{1}{2} \left(\sigma_{0d} + \frac{\sigma_{0b}}{L_b} \right) + \frac{1}{2} \sqrt{[\sigma_{0d} + (\sigma_{0b}/L_b)]^2 + 4(\tau_0/L_s)^2} \\ \sigma_2 &= \frac{1}{2} [\sigma_{0d} + (\sigma_{0b}/L_b)] - \frac{1}{2} \sqrt{[\sigma_{0d} + (\sigma_{0b}/L_b)]^2 + 4(\tau_0/L_s)^2} \end{aligned}$$

where σ_{0d} is the static axial stress and σ_{0b} is the static bending stress. Since $\sigma_3 = 0$, the formula for the von Mises theory is given by (Eq. 1.35)

$$\sigma_{eq} = \sqrt{\sigma_1^2 - \sigma_1 \sigma_2 + \sigma_2^2}$$

so that

$$n = \frac{\sigma_y}{\sigma_{eq}} = \frac{\sigma_y}{\sqrt{[\sigma_{0d} + (\sigma_{0b}/L_b)]^2 + 3(\tau_0/L_s)^2}} \quad (1.60)$$

1.10.2 Brittle Materials

It is customary to apply the full K_t factor in the design of members of brittle materials. The use of the full K_t factor for cast iron may be considered, in a sense, as penalizing this material unduly, since experiments show that the full effect is usually not obtained (Roark et al. 1938). The use of the full K_t factor may be partly justified as compensating, in a way, for the poor shock resistance of brittle materials. Since it is difficult to design rationally for shock or mishandling in transportation and installation, the larger sections obtained by the preceding rule may be a means of preventing some failures that might otherwise occur. However, notable designs of cast-iron members have been made (large paper-mill rolls, etc.) involving rather high stresses where full application of stress concentration factors would rule out this material. Such designs should be carefully made and may be viewed as exceptions to the rule. For ordinary design it seems wise to proceed cautiously in the treatment of notches in brittle materials, especially in critical load-carrying members.

The following factors of safety are based on the *maximum stress criterion* of failure of Section 1.8. For axial tension or bending (normal stress),

$$n = \frac{\sigma_{ut}}{K_t \sigma_0} \quad (1.61)$$

where σ_{ut} is the tensile ultimate strength, K_t is the stress concentration factor for normal stress, and σ_0 is the normal stress. For torsion of a round bar (shear stress),

$$n = \frac{\sigma_{ut}}{K_{ts}\tau_0} \quad (1.62)$$

where K_{ts} is the stress concentration factor for shear stress and τ_0 is the static shear stress.

The following factors of safety are based on *Mohr's theory* of failure of Section 1.8. Since the factors based on Mohr's theory are on the "safe side" compared to those based on the maximum stress criterion, they are suggested for design use. For axial tension or bending, Eq. (1.61) applies. For torsion of a round bar (shear stress), by Eq. (1.30),

$$n = \frac{\sigma_{ut}}{K_{ts}\tau_0} \left[\frac{1}{1 + (\sigma_{ut}/\sigma_{uc})} \right] \quad (1.63)$$

where σ_{ut} is the tensile ultimate strength and σ_{uc} is the compressive ultimate strength. For combined normal and shear stress,

$$n = \frac{2\sigma_{ut}}{K_t\sigma_0(1 - \sigma_{ut}/\sigma_{uc}) + (1 + \sigma_{ut}/\sigma_{uc})\sqrt{(K_t\sigma_0)^2 + 4(K_{ts}\tau_0)^2}} \quad (1.64)$$

1.11 DESIGN RELATIONS FOR ALTERNATING STRESS

1.11.1 Ductile Materials

For alternating (completely reversed cyclic) stress, the stress concentration effects must be considered. As explained in Section 1.9, the fatigue notch factor K_f is usually less than the stress concentration factor K_t . The factor K_{tf} represents a calculated estimate of the actual fatigue notch factor K_f . Naturally, if K_f is available from tests, one uses this, but a designer is very seldom in such a fortunate position. The expression for K_{tf} and K_{tsf} , Eqs. (1.53) and (1.54), respectively, are repeated here:

$$K_{tf} = q(K_t - 1) + 1 \quad (1.65)$$

$$K_{tsf} = q(K_{ts} - 1) + 1$$

The following expressions for factors of safety, are based on the von Mises criterion of failure as discussed in Section 1.8:

For axial or bending loading (normal stress),

$$n = \frac{\sigma_f}{K_{tf}\sigma_a} = \frac{\sigma_f}{[q(K_t - 1) + 1]\sigma_a} \quad (1.66)$$

where σ_f is the fatigue limit (endurance limit) in axial or bending test (normal stress) and σ_a is the alternating normal stress amplitude.

For torsion of a round bar (shear stress),

$$n = \frac{\tau_f}{K_{tsf}\tau_a} = \frac{\sigma_f}{\sqrt{3}K_{ts}\tau_a} = \frac{\sigma_f}{\sqrt{3}[q(K_{ts} - 1) + 1]\tau_a} \quad (1.67)$$

where τ_f is the fatigue limit in torsion and τ_a is the alternating shear stress amplitude.

For combined normal stress and shear stress,

$$n = \frac{\sigma_f}{\sqrt{(K_{tf}\sigma_a)^2 + 3(K_{tsf}\tau_a)^2}} \quad (1.68)$$

By rearranging Eq. (1.68), the equation for an ellipse is obtained,

$$\frac{\sigma_a^2}{(\sigma_f/nK_{tf})^2} + \frac{\tau_a^2}{(\sigma_f/n\sqrt{3}K_{tsf})^2} = 1 \quad (1.69)$$

where $\sigma_f/(nK_{tf})$ and $\sigma_f/(n\sqrt{3}K_{tsf})$ are the major and minor semiaxes. Fatigue tests of unnotched specimens by Gough and Pollard (1935) and by Nisihara and Kawamoto (1940) are in excellent agreement with the elliptical relation. Fatigue tests of notched specimens (Gough and Clenshaw 1951) are not in as good agreement with the elliptical relation as are the unnotched, but for design purposes the elliptical relation seems reasonable for ductile materials.

1.11.2 Brittle Materials

Since our knowledge in this area is very limited, it is suggested that unmodified K_t factors be used. Mohr's theory of Section 1.8, with $\sigma_{ut}/\sigma_{uc} = 1$, is suggested for design purposes for brittle materials subjected to alternating stress.

For axial or bending loading (normal stress),

$$n = \frac{\sigma_f}{K_t\sigma_a} \quad (1.70)$$

For torsion of a round bar (shear stress),

$$n = \frac{\tau_f}{K_{ts}\tau_a} = \frac{\sigma_f}{2K_{ts}\tau_a} \quad (1.71)$$

For combined normal stress and shear stress,

$$n = \frac{\sigma_f}{\sqrt{(K_t\sigma_a)^2 + 4(K_{ts}\tau_a)^2}} \quad (1.72)$$

1.12 DESIGN RELATIONS FOR COMBINED ALTERNATING AND STATIC STRESSES

The majority of important strength problems comprises neither simple static nor alternating cases, but involves fluctuating stress, which is a combination of both. A cyclic fluctuating stress (Fig. 1.33) having a maximum value σ_{\max} and minimum value σ_{\min} can be considered as having an *alternating component* of amplitude

$$\sigma_a = \frac{\sigma_{\max} - \sigma_{\min}}{2} \quad (1.73)$$

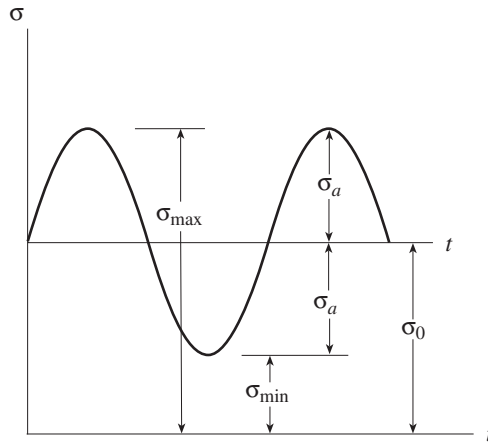


Figure 1.33 Combined alternating and steady stresses.

and a *steady or static component*

$$\sigma_0 = \frac{\sigma_{\max} + \sigma_{\min}}{2} \quad (1.74)$$

1.12.1 Ductile Materials

In designing parts to be made of ductile materials for normal temperature use, it is the usual practice to apply the stress concentration factor to the alternating component but not to the static component. This appears to be a reasonable procedure and is in conformity with test data (Houdremont and Bennek 1932) such as that shown in Fig. 1.34a. The limitations discussed in Section 1.10 still apply.

By plotting minimum and maximum limiting stresses in Fig. 1.34a, the relative positions of the static properties, such as yield strength and tensile strength, are clearly shown. However, one can also use a simpler representation such as that of Fig. 1.34b, with the alternating component as the ordinate.

If, in Fig. 1.34a, the curved lines are replaced by straight lines connecting the end points σ_f and σ_u , σ_f/K_{tf} and σ_u , we have a simple approximation which is on the safe side for steel members.⁸ From Fig. 1.34b we can obtain the following simple rule for factor of safety:

$$n = \frac{1}{(\sigma_0/\sigma_u) + (K_{tf}\sigma_a/\sigma_f)} \quad (1.75)$$

This is the same as the following Soderberg rule (Pilkey 2005), except that σ_u is used instead of σ_y . Soderberg's rule is based on the yield strength (see lines in Fig. 1.34

⁸For steel members, a cubic relation (Peterson 1952; Nichols 1969) fits available data fairly well, $\sigma_a = [\sigma_f/(7K_{tf})]\{8 - [(\sigma_0/\sigma_u) + 1]^3\}$. This is the equation for the lower full curve of Fig. 1.34b. For certain aluminum alloys, the σ_a, σ_0 curve has a shape (Lazan and Blatherwick 1952) that is concave slightly below the $\sigma_f/K_f, \sigma_u$ line at the upper end and is above the line at the lower end.

connecting σ_f and σ_y , σ_f/K_{tf} and σ_y):

$$n = \frac{1}{(\sigma_0/\sigma_y) + (K_{tf}\sigma_a/\sigma_f)} \quad (1.76)$$

By referring to Fig. 1.34b, it can be shown that $n = OB/OA$. Note that in Fig. 1.34a, the pulsating (0 to max) condition corresponds to $\tan^{-1} 2$, or 63.4° , which in Fig. 1.34b is 45° .

Equation (1.76) may be further modified to be in conformity with Eqs. (1.56) and (1.57), which means applying limit design for yielding, with the factors and considerations as stated in Section 1.10.1:

$$n = \frac{1}{(\sigma_{0d}/\sigma_y) + (\sigma_{0b}/L_b\sigma_y) + (K_{tf}\sigma_a/\sigma_f)} \quad (1.77)$$

As mentioned previously $L_b\sigma_y$ must not exceed σ_u . That is, the factor of safety n from Eq. (1.77) must not exceed n from Eq. (1.75).

For torsion, the same assumptions and use of the von Mises criterion result in:

$$n = \frac{1}{\sqrt{3} [(\tau_0/L_s\sigma_y) + (K_{tsf}\tau_a/\sigma_f)]} \quad (1.78)$$

For notched specimens Eq. (1.78) represents a design relation, being on the safe edge of test data (Smith 1942). It is interesting to note that, for unnotched torsion specimens, static torsion (up to a maximum stress equal to the yield strength in torsion) does not lower the limiting alternating torsional range. It is apparent that further research is needed in the torsion region; however, since notch effects are involved in design (almost without exception), the use of Eq. (1.78) is indicated. Even in the absence of stress concentration, Eq. (1.78) would be on the "safe side," though by a large margin for relatively large values of statically applied torque.

For a combination of *static (steady) and alternating normal stresses plus static and alternating shear stresses* (alternating components in phase) the following relation, derived by Soderberg (1930), is based on expressing the shear stress on an arbitrary plane in terms of static and alternating components, assuming failure is governed by the maximum shear theory and a "straight-line" relation similar to Eq. (1.76) and finding the plane that gives a minimum factor of safety n (Peterson 1953):

$$n = \frac{1}{\sqrt{[(\sigma_0/\sigma_y) + (K_t\sigma_a/\sigma_f)]^2 + 4 [(\tau_0/\sigma_y) + (K_{ts}\tau_a/\sigma_f)]^2}} \quad (1.79)$$

The following modifications are made to correspond to the end conditions represented by Eqs. (1.56), (1.57), (1.59), (1.66), and (1.67). Then Eq. (1.79) becomes

$$n = \frac{1}{\sqrt{[(\sigma_{0d}/\sigma_y) + (\sigma_{0b}/L_b\sigma_y) + (K_{tf}\sigma_a/\sigma_f)]^2 + 3 [(\tau_0/L_s\sigma_y) + (K_{tsf}\tau_a/\sigma_f)]^2}} \quad (1.80)$$

For steady stress only, Eq. (1.80) reduces to Eq. (1.60).

For alternating stress only, Eq. (1.80) reduces to Eq. (1.68).

For normal stress only, Eq. (1.80) reduces to Eq. (1.77).

For torsion only, Eq. (1.80) reduces to Eq. (1.78).

In tests by Ono (1921, 1929) and by Lea and Budgen (1926) the alternating bending fatigue strength was found not to be affected by the addition of a static (steady) torque (less than the yield torque). Other tests reported in a discussion by Davies (1935) indicate a lowering of the bending fatigue strength by the addition of static torque. Hohenemser and Prager (1933) found that a static tension lowered the alternating torsional fatigue strength; Gough and Clenshaw (1951) found that steady bending lowered the torsional fatigue strength of plain specimens but that the effect was smaller for specimens involving stress concentration. Further experimental work is needed in this area of special combined stress combinations, especially in the region involving the additional effect of stress concentration. In the meantime, while it appears that use of Eq. (1.80) may be overly “safe” in certain cases of alternating bending plus steady torque, it is believed that Eq. (1.80) provides a reasonable general design rule.

1.12.2 Brittle Materials

A “straight-line” simplification similar to that of Fig. 1.34 and Eq. (1.75) can be made for brittle material, except that the stress concentration effect is considered to apply also to the static (steady) component.

$$n = \frac{1}{K_t [(\sigma_0/\sigma_{ut}) + (\sigma_a/\sigma_f)]} \quad (1.81)$$

As previously mentioned, unmodified K_t factors are used for the brittle material cases.

For *combined shear and normal stresses*, data are very limited. For combined alternating bending and static torsion, Ono (1921) reported a decrease of the bending fatigue strength of cast iron as steady torsion was added. By use of the Soderberg method (Soderberg 1930) and basing failure on the normal stress criterion (Peterson 1953), we obtain

$$n = \frac{2}{K_t \left(\frac{\sigma_0}{\sigma_{ut}} + \frac{\sigma_a}{\sigma_f} \right) + \sqrt{K_t^2 \left(\frac{\sigma_0}{\sigma_{ut}} + \frac{\sigma_a}{\sigma_f} \right)^2 + 4K_{ts}^2 \left(\frac{\tau_0}{\sigma_{ut}} + \frac{\tau_a}{\sigma_f} \right)^2}} \quad (1.82)$$

A rigorous formula for combining Mohr’s theory components of Eqs. (1.64) and (1.72) does not seem to be available. The following approximation which satisfies Eqs. (1.61), (1.63), (1.70), and (1.71) may be of use in design, in the absence of a more exact formula.

$$n = \frac{2}{K_t \left(\frac{\sigma_0}{\sigma_{ut}} + \frac{\sigma_a}{\sigma_f} \right) \left(1 - \frac{\sigma_{ut}}{\sigma_{uc}} \right) + \left(1 + \frac{\sigma_{ut}}{\sigma_{uc}} \right) \sqrt{K_t^2 \left(\frac{\sigma_0}{\sigma_{ut}} + \frac{\sigma_a}{\sigma_f} \right)^2 + 4K_{ts}^2 \left(\frac{\tau_0}{\sigma_{ut}} + \frac{\tau_a}{\sigma_f} \right)^2}} \quad (1.83)$$

For steady stress only, Eq. (1.83) reduces to Eq. (1.64).

For alternating stress only, with $\sigma_{ut}/\sigma_{uc} = 1$, Eq. (1.83) reduces to Eq. (1.72).

For normal stress only, Eq. (1.83) reduces to Eq. (1.81).

For torsion only, Eq. (1.83) reduces to

$$n = \frac{1}{K_{ts} \left(\frac{\tau_0}{\sigma_{ut}} + \frac{\tau_a}{\sigma_f} \right) \left(1 + \frac{\sigma_{ut}}{\sigma_{uc}} \right)} \quad (1.84)$$

This in turn can be reduced to the component cases of Eqs. (1.63) and (1.71).

1.13 LIMITED NUMBER OF CYCLES OF ALTERNATING STRESS

In *Stress Concentration Design Factors* (1953), Peterson presented formulas for a limited number of cycles (upper branch of the S-N diagram). These relations were based on an average of available test data and therefore apply to polished test specimens 0.2 to 0.3 in. diameter. If the member being designed is not too far from this size range, the formulas may be useful as a rough guide, but otherwise they are questionable, since the number of cycles required for a crack to propagate to rupture of a member depends on the size of the member.

Fatigue failure consists of three stages: crack initiation, crack propagation, and rupture. Crack initiation is thought not to be strongly dependent on size, although from statistical considerations of the number of “weak spots,” one would expect some effect. So much progress has been made in the understanding of crack propagation under cyclic stress, that it is believed that reasonable estimates can be made for a number of problems.

1.14 STRESS CONCENTRATION FACTORS AND STRESS INTENSITY FACTORS

Consider an elliptical hole of major axis $2a$ and minor axis $2b$ in a plane element (Fig. 1.35a). If $b \rightarrow 0$ (or $a \gg b$), the elliptical hole becomes a crack of length $2a$ (Fig. 1.35b). The *stress intensity factor* K represents the strength of the elastic stress fields surrounding the crack tip (Pilkey 2005). It would appear that there might be a relationship between the stress concentration factor and the stress intensity factor. Creager and Paris (1967) analyzed the stress distribution around the tip of a crack of length $2a$ using the coordinates shown in Fig. 1.36. The origin O of the coordinates is set a distance of $r/2$ from the tip, in which r is the radius of curvature of the tip. The stress σ_y in the y direction near the tip can be expanded as a power series in terms of the radial distance. Discarding all terms higher than second order, the approximation for mode I fracture (Pilkey 2005, Sec. 7.2) becomes

$$\sigma_y = \sigma + \frac{K_I}{\sqrt{2\pi\rho}} \frac{r}{2\rho} \cos \frac{3\theta}{2} + \frac{K_I}{\sqrt{2\pi\rho}} \cos \frac{\theta}{2} \left(1 + \sin \frac{\theta}{2} \sin \frac{3\theta}{2} \right) \quad (1.85)$$

where σ is the tensile stress remote from the crack, (ρ, θ) are the polar coordinates of the crack tip with origin O (Fig. 1.36), K_I is the mode I stress intensity factor of the case

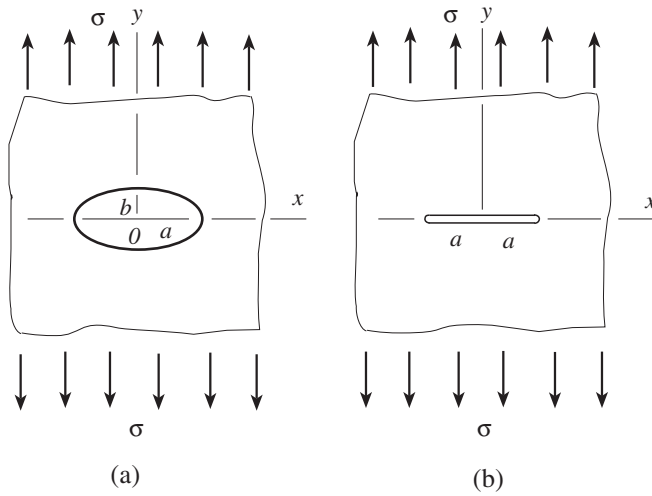


Figure 1.35 Elliptic hole model of a crack as $b \rightarrow 0$: (a) elliptic hole; (b) crack.

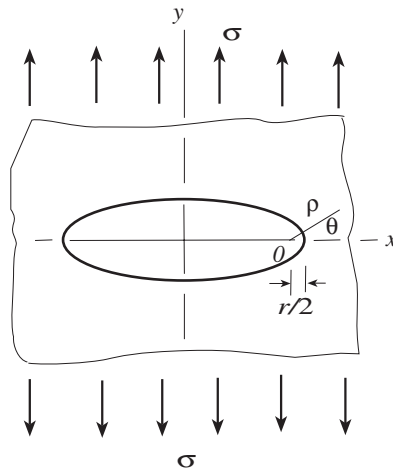


Figure 1.36 Coordinate system for stress at the tip of an ellipse.

in Fig. 1.35b. The maximum longitudinal stress occurs at the tip of the crack, that is, at $\rho = r/2, \theta = 0$. Substituting this condition into Eq. (1.85) gives

$$\sigma_{\max} = \sigma + 2 \frac{K_I}{\sqrt{\pi r}} \tag{1.86}$$

However, the stress intensity factor can be written as (Pilkey 2005)

$$K_I = C\sigma\sqrt{\pi a} \tag{1.87}$$

where C is a constant that depends on the shape and the size of the crack and the specimen.

Substituting Eq. (1.87) into Eq. (1.86), the maximum stress is

$$\sigma_{\max} = \sigma + 2C\sigma\sqrt{\frac{a}{r}} \tag{1.88}$$

With σ as the reference stress, the stress concentration factor at the tip of the crack for a two-dimensional element subjected to uniaxial tension is

$$K_t = \frac{\sigma_{\max}}{\sigma_{\text{nom}}} = 1 + 2C\sqrt{\frac{a}{r}} \tag{1.89}$$

Equation (1.89) gives an approximate relationship between the stress concentration factor and the stress intensity factor. Due to the rapid development of fracture mechanics, a large number of crack configurations have been analyzed, and the corresponding results can be found in various handbooks. These results may be used to estimate the stress concentration factor for many cases. For instance, for a crack of length $2a$ in an infinite element under uniaxial tension, the factor C is equal to 1, so the corresponding stress concentration factor is

$$K_t = \frac{\sigma_{\max}}{\sigma_{\text{nom}}} = 1 + 2\sqrt{\frac{a}{r}} \tag{1.90}$$

Eq. (1.90) is the same as found in Chapter 4 (Eq. 4.58) for the case of a single elliptical hole in an infinite element in uniaxial tension. It is not difficult to apply Eq. (1.89) to other cases.

Example 1.8 *Element with a Circular Hole with Opposing Semicircular Lobes*

Find the stress concentration factor of an element with a hole of diameter d and opposing semicircular lobes of radius r as shown in Fig. 1.37, which is under uniaxial tensile stress σ . Use known stress intensity factors. Suppose that $a/H = 0.1$, $r/d = 0.1$.

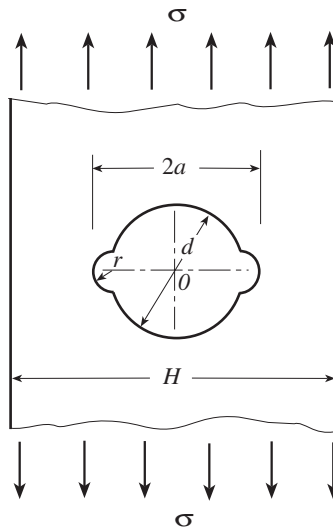


Figure 1.37 Element with a circular hole with two opposing semicircular lobes.

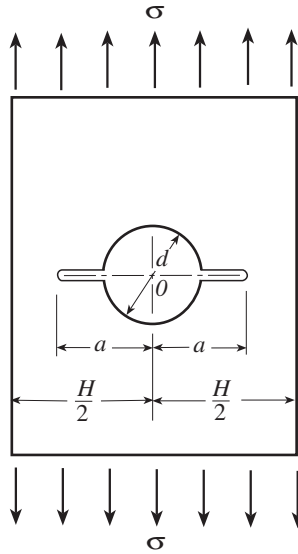


Figure 1.38 Element with a circular hole and a pair of equal length cracks.

For this problem, choose the stress intensity factor for the case of radial cracks emanating from a circular hole in a rectangular panel as shown in Fig. 1.38. From Sih (1973) it is found that $C = 1.0249$ when $a/H = 0.1$. The crack length is $a = d/2 + r$ and $r/d = 0.1$, so

$$\frac{a}{r} = \frac{d/2 + r}{r} = 1 + \frac{d}{2r} = 1 + \frac{1}{2 \times 0.1} = 6 \quad (1)$$

Substitute $C = 1.0249$ and $a/r = 6$ into Eq. (1.89),

$$K_t = 1 + 2 \cdot 1.0249 \cdot \sqrt{6} = 6.02 \quad (2)$$

The stress concentration factor for this case also can be found from Chart 4.61. Corresponding to $a/H = 0.1$, $r/d = 0.1$, the stress concentration factor based on the net area is

$$K_m = 4.80 \quad (3)$$

The stress concentration factor based on the gross area is (Example 1.1)

$$K_{tg} = \frac{K_m}{1 - (d/H)} = \frac{4.80}{1 - 0.2} = 6.00 \quad (4)$$

The results of (2) and (4) are very close.

Further results are listed below. It would appear that this kind of approximation is reasonable.

H	r/d	K_t from Eq. (1.89)	K_{tg} from Chart 4.61	% Difference
0.2	0.05	7.67	7.12	7.6
0.2	0.25	4.49	4.6	-2.4
0.4	0.1	6.02	6.00	0.33
0.6	0.1	6.2	6.00	0.3
0.6	0.25	4.67	4.7	-0.6

Shin et al. (1994) compared the use of Eq. (1.89) with the stress concentration factors obtained from handbooks and the finite element method. The conclusion is that in the range of practical engineering geometries where the notch tip is not too close to the boundary line of the element, the discrepancy is normally within 10%. Table 1.2 provides a comparison for a case in which two identical parallel ellipses in an infinite element are not aligned in the axial loading direction (Fig. 1.39).

TABLE 1.2 Stress Concentration Factors for the Configurations of Fig. 1.39

a/l	a/r	e/f	C	K_t	K_t from Eq (1.89)	Discrepancy (90%)
0.34	87.1	0.556	0.9	17.84	17.80	-0.2
0.34	49	0.556	0.9	13.38	13.60	1.6
0.34	25	0.556	0.9	9.67	10.00	3.4
0.34	8.87	0.556	0.9	6.24	6.36	1.9
0.114	0.113	1.8	1.01	1.78	1.68	-6.0

Sources: Values for C from Shin et al. (1994); values for K_t from Murakami (1987).

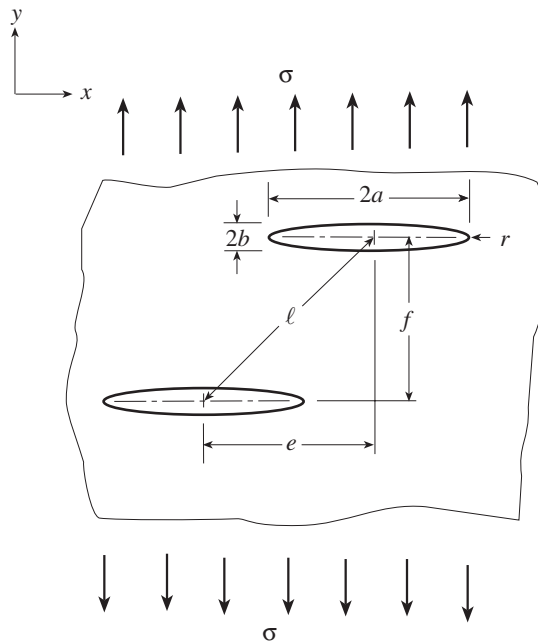


Figure 1.39 Infinite element with two identical ellipses that are not aligned in the y direction.

REFERENCES

- ASTM, 1994, *Annual Book of ASTM Standards*, Vol. 03.01, American Society for Testing and Materials, Philadelphia, PA.
- Boresi, A. P., Schmidt, R. J., and Sidebottom, O. M., 1993, *Advanced Mechanics of Materials*, 5th ed., Wiley, New York.
- Cox, H. L., and Sopwith, D. G., 1937, The effect of orientation on stresses in single crystals and of random orientation on the strength of polycrystalline aggregates, *Proc. Phys. Soc. London*, Vol. 49, p. 134.
- Creager, M., and Paris, P. C., 1967, Elastic field equations for blunt cracks with reference to stress corrosion cracking, *Int. J. Fract. Mech.*, Vol. 3, pp. 247–252.
- Davies, V. C., 1935, Discussion based on theses of S. K. Nimhanmimie and W. J. Huitt (Battersea Polytechnic), *Proc. Inst. Mech. Eng. London*, Vol. 131, p. 66.
- Davis, E. A., and Manjoine, M. J., 1952, Effect of notch geometry on rupture strength at elevated temperature, *Proc. ASTM*, Vol. 52.
- Draffin, J. O., and Collins, W. L., 1938, Effect of size and type of specimens on the torsional properties of cast iron, *Proc. ASTM*, Vol. 38, p. 235.
- Durelli, A. J., 1982, *Stress Concentrations*, U.M. Project SF-CARS, School of Engineering, University of Maryland, Office of Naval Research, Washington, DC.
- Eichinger, A., 1926, Versuche zur Klärung der Frage der Bruchgefahr, *Proc. 2nd International Congress on Applied Mechanics*, Zurich, Switzerland, p. 325.
- Findley, W. N., 1951, Discussion of “Engineering steels under combined cyclic and static stresses” by H. J. Gough, 1949, *Trans. ASME Appl. Mech. Sect.*, Vol. 73, p. 211.
- Fralich, R. W., 1959, Experimental investigation of effects of random loading on the fatigue life of notched cantilever beam specimens of 7075-T6 aluminum alloy, *NASA Memo 4-12-59L*, National Aeronautics and Space Administration, Washington, DC.
- Gough, H. J., 1933, Crystalline structure in relation to failure of metals, *Proc. ASTM*, Vol. 33, Pt. 2, p. 3.
- Gough, H. J., and Clenshaw, W. J., 1951, Some experiments on the resistance of metals to fatigue under combined stresses, *ARC R&M 2522*, Aeronautical Research Council, London.
- Gough, H. J., and Pollard, H. V., 1935, Strength of materials under combined alternating stress, *Proc. Inst. Mech. Eng. London*, Vol. 131, p. 1, Vol. 132, p. 549.
- Gunn, N. J. R., 1952, Fatigue properties at low temperature on transverse and longitudinal notched specimens of DTD363A aluminum alloy, *Tech. Note Met. 163*, Royal Aircraft Establishment, Farnborough, England.
- Hencky, H., 1924, Zur Theorie plastischer Deformationen und der Hierdurch im Material hervorgerufenen Nebenspannungen, *Proc. 1st International Congress on Applied Mechanics*, Delft, The Netherlands, p. 312.
- Hohenemser, K., and Prager, W., 1933, Zur Frage der Ermüdungsfestigkeit bei mehrachsigen Spannungszuständen, *Metall*, Vol. 12, p. 342.
- Houdremont, R., and Bennek, H., 1932, Federstähle, *Stahl Eisen*, Vol. 52, p. 660.
- Howland, R. C. J., 1930, On the stresses in the neighborhood of a circular hole in a strip under tension, *Trans. R. Soc. London Ser. A*, Vol. 229, p. 67.
- Ku, T.-C., 1960, Stress concentration in a rotating disk with a central hole and two additional symmetrically located holes, *J. Appl. Mech.*, Vol. 27, Ser. E, No. 2, pp. 345–360.
- Kuhn, P., and Hardrath, H. F., 1952, An engineering method for estimating notch-size effect in fatigue tests of steel, *NACA Tech. Note 2805*, National Advisory Committee on Aeronautics, Washington, DC.

- Lazan, B. J., and Blatherwick, A. A., 1952, Fatigue properties of aluminum alloys at various direct stress ratios, *WADC TR 52-306 Part I*, Wright-Patterson Air Force Base, Dayton, OH.
- Lazan, B. J., and Blatherwick, A. A., 1953, Strength properties of rolled aluminum alloys under various combinations of alternating and mean axial stresses, *Proc. ASTM*, Vol. 53, p. 856.
- Lea, F. C., and Budgen, H. P., 1926, Combined torsional and repeated bending stresses, *Engineering London*, Vol. 122, p. 242.
- Leven, M. M., 1955, Quantitative three-dimensional photoelasticity, *Proc. SESA*, Vol. 12, No. 2, p. 167.
- Little, R. W., 1973, *Elasticity*, Prentice-Hall, Englewood Cliffs, NJ, p. 160.
- Ludwik, P., 1931, Kerb- und Korrosionsdauerfestigkeit, *Metall*, Vol. 10, p. 705.
- Marin, J., 1952, *Engineering Materials*, Prentice-Hall, Englewood Cliffs, NJ.
- Murakami, Y., 1987, *Stress Intensity Factor Handbook*, Pergamon Press, Elmsford, NY.
- Nadai, A., 1937, Plastic behavior of metals in the strain hardening range," *J. Appl. Phys.*, Vol. 8, p. 203.
- Neuber, H., 1958, *Kerbspannungslehre*, 2nd ed. (in German), Springer-Verlag, Berlin; translation, 1961, *Theory of Notch Stresses*, Office of Technical Services, U.S. Department of Commerce, Washington, DC, 1961 p. 207.
- Neuber, H., 1968, Theoretical determination of fatigue strength at stress concentration, *Rep. AFML-TR-68-20*, Air Force Materials Laboratory, Wright-Patterson Air Force Base, Dayton, OH.
- Newmark, N. M., Mosborg, R. J., Munse, W. H., and Elling, R. E., 1951, Fatigue tests in axial compression, *Proc. ASTM*, Vol. 51, p. 792.
- Newton, R. E., 1940, A photoelastic study of stresses in rotating disks, *J. Appl. Mech.*, Vol. 7, p. 57.
- Nichols, R. W., Ed., 1969, *A Manual of Pressure Vessel Technology*, Elsevier, London, Chap. 3.
- Nishida, M., 1976, *Stress Concentration*, Mori Kita Press, Tokyo (in Japanese).
- Nisihara, T., and Kawamoto, A., 1940, The strength of metals under combined alternating stresses, *Trans. Soc. Mech. Eng. Jpn.*, Vol. 6, No. 24, p. S-2.
- Nisihara, T., and Kojima, K., 1939, Diagram of endurance limit of duralumin for repeated tension and compression, *Trans. Soc. Mech. Eng. Jpn.*, Vol. 5, No. 20, p. I-1.
- Ono, A., 1921, Fatigue of steel under combined bending and torsion, *Mem. Coll. Eng. Kyushu Imp. Univ.*, Vol. 2, No. 2.
- Ono, A., 1929, Some results of fatigue tests of metals, *J. Soc. Mech. Eng. Jpn.*, Vol. 32, p. 331.
- Peterson, R. E., 1933a, Stress concentration phenomena in fatigue of metals, *Trans. ASME Appl. Mech. Sect.*, Vol. 55, p. 157.
- Peterson, R. E., 1933b, Model testing as applied to strength of materials, *Trans. ASME Appl. Mech. Sect.*, Vol. 55, p. 79.
- Peterson, R. E., 1938, Methods of correlating data from fatigue tests of stress concentration specimens, *Stephen Timoshenko Anniversary Volume*, Macmillan, New York, p. 179.
- Peterson, R. E., 1943, Application of stress concentration factors in design, *Proc. Soc. Exp. Stress Anal.*, Vol. 1, No. 1, p. 118.
- Peterson, R. E., 1945, Relation between life testing and conventional tests of materials, *ASTA Bull.*, p. 13.
- Peterson, R. E., 1950, Relation between stress analysis and fatigue of metals, *Proc. Soc. Exp. Stress Anal.*, Vol. 11, No. 2, p. 199.
- Peterson, R. E., 1952, Brittle fracture and fatigue in machinery, in *Fatigue and Fracture of Metals*, Wiley, New York, p. 74.
- Peterson, R. E., 1953, *Stress Concentration Design Factors*, Wiley, New York.
- Peterson, R. E., 1959, Analytical approach to stress concentration effect in aircraft materials, *Tech. Rep. 59-507*, U.S. Air Force-WADC Symposium on Fatigue of Metals, Dayton, OH, p. 273.

- Peterson, R. E., 1974, *Stress Concentration Factors*, Wiley, New York.
- Peterson, R. E., and Wahl, A. M., 1936, Two and three dimensional cases of stress concentration and comparison with fatigue tests, *Trans. ASME Appl. Mech. Sect.*, Vol. 57, p. A-15.
- Pilkey, W. D., 2005, *Formulas for Stress, Strain, and Structural Matrices*, 2nd ed., Wiley, Hoboken, NJ.
- Pilkey, W. D., and Wunderlich, W., 1993, *Mechanics of Structures: Variational and Computational Methods*, CRC Press, Boca Raton, FL.
- Prager, W., and Hodge, P. G., 1951, *Theory of Perfectly Plastic Solids*, Wiley, New York.
- Roark, R. J., Hartenberg, R. S., and Williams, R. Z., 1938, The influence of form and scale on strength, *Univ. Wisc. Exp. Stn. Bull.* 84.
- Rös, M., and Eichinger, A., 1950, Die Bruchgefahr fester Körper, *Eidg. Materialpruef. Ber.*, Vol. 173.
- Sachs, G., 1928, Zur Ableitung einer Fließbedingung, *Z. VDI*, Vol. 72, p. 734.
- Shin, C. S., Man, K. C., and Wang, C. M., 1994, A practical method to estimate the stress concentration of notches, *Int. J. Fatigue*, Vol. 16, No. 4, pp. 242–256.
- Sih, G. C., 1973, *Handbook of Stress Intensity Factors*, Lehigh University, Bethlehem, PA.
- Smith, J. O., 1942, The effect of range of stress on the fatigue strength of metals, *Univ. Ill. Exp. Stn. Bull.* 334.
- Soderberg, C. R., 1930, Working stress, *Trans. ASME*, Vol. 52, Pt. 1, p. APM 52–2.
- Steele, M. C., Liu, C. K., and Smith, J. O., 1952, Critical review and interpretation of the literature on plastic (inelastic) behavior of engineering metallic materials, research report, Department of Theoretical and Applied Mechanics, University of Illinois, Urbana, IL.
- Templin, R. L., 1954, Fatigue of aluminum, *Proc. ASTM*, Vol. 54, p. 641.
- Timoshenko, S., and Goodier, J. N., 1970, *Theory of Elasticity*, McGraw-Hill, New York.
- Van den Broek, J. A., 1942, *Theory of Limit Design*, Wiley, New York.
- Von Mises, R., 1913, Mechanik der festen Körper im plastisch deformablen Zustand, *Nachr. Ges. Wiss. Goettingen Jahresber. Geschaeftsjahr. Math.-phys. Kl.*, p. 582.
- Von Philipp, H. A., 1942, Einfluss von Querschnittsgröße und Querschnittsform auf die Dauerfestigkeit bei ungleichmäßig verteilten Spannungen, *Forschung*, Vol. 13, p. 99.

Sources of Stress Concentration Factors

- Neuber, H., 1958, *Theory of Notch Stresses*, 2nd ed., Springer-Verlag, Berlin; translation, 1961, Office of Technical Services, U.S. Department of Commerce, Washington, DC.
- Nishida, M., 1976, *Stress Concentration*, Mori Kita Press, Tokyo (in Japanese).
- Pilkey, W. D., 2005, *Formulas for Stress, Strain, and Structural Matrices*, 2nd ed., Wiley, Hoboken, NJ.
- Savin, G. N., 1961, *Stress Concentration Around Holes*, Pergamon Press, London (English translation editor, W. Johnson).
- Savin, G. N., and Tulchii, V. I., 1976, *Handbook on Stress Concentration*, Higher Education Publishing House (Chinese translation, Heilongjiang Science and Technology Press, Harbin, China).
- Young, W. C., 1989, *Roark's Formulas for Stress and Strain*, 7th ed., McGraw-Hill, New York.

Web Site for This Book

www.stressconcentrationfactors.com, discussion forums and errata related to this book.